Design of a Modular Multi-Finger Grip-Force Measurement System for Post-Stroke Hand Function Assessment

By

Jasper van Aernsbergen

In partial fulfilment of the requirements for the degree of
Master of Science
at Delft University of Technology,
to be defended publicly on Monday, 15 December, 2025 at 10.45

Faculty: Mechanical Engineering
Department: BioMechanical Engineering
Programme: ME-BMD

Mentors / Supervisors: Dr. Ir. A.H.A. Stienen,
Ir. J.C. van Zanten (Daily, PhDc)

Graduation committee: Dr. Ir. A.H.A. Stienen (Chair),
Ir. J.C. van Zanten,
Prof. Dr. Ir. F.C.T. van der Helm

An electronic version of this thesis is available at http://repository.tudelft.nl

TU Delft

Keywords:
Hand-function assessment,
Finger-force measurement,
Design Thinking,
Modular grasp device,
Rehabilitation technology,
Post-stroke

Abstract
Background and Objective — Accurate measurement of individual finger forces is essential for assessing hand function and understanding motor impairments, yet conventional tools such as dynamometers measure only total grip strength and offer no insight into finger-specific contributions. This thesis addresses this gap by designing and validating a modular measurement system capable of measuring forces from all five digits across three predefined grasp types, operable by post-stroke patients and compatible with integration into perturbation platforms such as the Shoulder–Elbow Perturbator (SEP).

Methods and Results — An iterative Design Thinking approach guided the development of a modular hand-function assessment device featuring interchangeable grasp interfaces with spring-guided pistons to enable natural grasp motion while capturing individual finger forces. Sensor calibration using standardized weight steps showed excellent linearity, with an average calibration error of 0.15 N, substantially outperforming the 1.25 N error specified by the manufacturer. Validation with thirteen healthy participants demonstrated high repeatability across all grasp types, with SD, CV, and RMSE values comparable to a reference dynamometer. The device further reproduced expected biomechanical force-distribution patterns, including the characteristic flattening of finger contributions in larger cylindrical grasps.

Conclusion — The results demonstrate the feasibility of a practical, compact, and modular multi-finger force measurement system capable of detailed hand-function assessment. With refinement of mechanical tolerances and subsequent clinical validation, the device has strong potential for both rehabilitation assessment and integration into perturbation-based motor-control research, providing a more complete understanding of individual finger contributions during functional grasping.

Design of a Modular Multi-Finger Grip-Force Measurement System for Post-Stroke Hand Function Assessment

Design, Implementation, and Prototype Validation

Jasper van Aernsbergen, 5158990

Supervisors: Jonathan van Zanten (daily), Arno Stienen

Department of BioMechanical Engineering
Delft University of Technology, Delft, The Netherlands

***Abstract*— *Background and Objective*— Accurate measurement of individual finger forces is essential for assessing hand function and understanding motor impairments, yet conventional tools such as dynamometers measure only total grip strength and offer no insight into finger-specific contributions. This thesis addresses this gap by designing and validating a modular measurement system capable of measuring forces from all five digits across three predefined grasp types, operable by post-stroke patients and compatible with integration into perturbation platforms such as the Shoulder–Elbow Perturbator (SEP).**

***Methods and Results*— An iterative Design Thinking approach guided the development of a modular hand-function assessment device featuring interchangeable grasp interfaces with spring-guided pistons to enable natural grasp motion while capturing individual finger forces. Sensor calibration using standardized weight steps showed excellent linearity, with an average calibration error of 0.15 N, substantially outperforming the 1.25 N error specified by the manufacturer. Validation with thirteen healthy participants demonstrated high repeatability across all grasp types, with SD, CV, and RMSE values comparable to a reference dynamometer. The device further reproduced expected biomechanical force-distribution patterns, including the characteristic flattening of finger contributions in larger cylindrical grasps.**

***Conclusion*— The results demonstrate the feasibility of a practical, compact, and modular multi-finger force measurement system capable of detailed hand-function assessment. With refinement of mechanical tolerances and subsequent clinical validation, the device has strong potential for both rehabilitation assessment and integration into perturbation-based motor-control research, providing a more complete understanding of individual finger contributions during functional grasping.**

***Index Terms*— Hand-function assessment, finger-force measurement, Design Thinking, modular grasp device, rehabilitation technology, post-stroke**

I. Introduction

A. Background and motivation

Stroke, also known as a Cerebrovascular Accident (CVA), is one of the leading causes of death and long-term disability worldwide [1]. Between 1990 and 2021, the global incidence of stroke increased by 70%, while stroke-related mortality rose by 44%. As survival rates improve, the number of people living with stroke-related disabilities continues to grow.

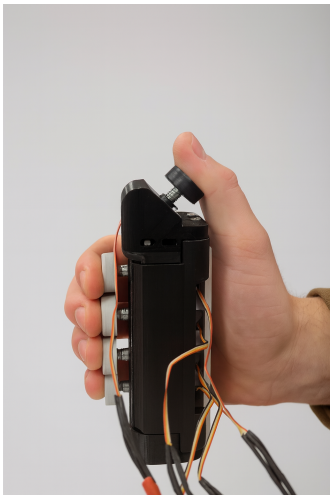

Fig. 1: Prototype of the modular grip-force measurement system developed in this thesis, shown here configured for the Medium Wrap grasp

A common consequence of stroke is impairment of the upper limb [2], typically characterized by muscle weakness, spasticity, and abnormal muscle synergies [3]. Spasticity refers to a velocity-dependent increase in muscle tone caused by an exaggerated stretch reflex [4], whereas abnormal muscle synergies reflect the pathological coupling of joint movements due to disrupted neural control [5]. These deficits compromise a patient's ability to perform activities of daily living (ADLs), including reaching, grasping, and manipulating objects [6].

Beyond the loss of strength, many stroke survivors experience reduced force control, defined as the ability to generate and maintain muscle force accurately and steadily [7]. Impaired force modulation decreases the precision and stability of grasping tasks and highlights the need for measurement systems that capture not only maximum strength but also fine force regulation during functional hand movements.

Among upper-limb impairments, loss of hand function is particularly disabling [8]. Up to 87% of stroke survivors experience partial or complete paralysis of one or more fingers

[9], severely limiting fine motor dexterity and personal independence. Accurate assessment of hand function is therefore essential for planning rehabilitation and monitoring recovery trajectories [10]. However, widely used clinical scales such as the Modified Ashworth Scale (MAS), Modified Tardieu Scale (MTS), and Fugl–Meyer Assessment (FMA) provide only qualitative or ordinal insight into hand performance and lack the resolution required to characterize finger-specific coordination, strength, and control [11]. Measuring the forces generated by individual fingers is essential, as studies have shown that finger-specific strength and force distribution strongly influence hand function outcomes and cannot be captured by overall hand-grip measurements alone [12].

B. Gap

Assessment of hand function is a key component of post-stroke rehabilitation, yet existing clinical and research tools remain limited. Conventional clinical tools, such as hand dynamometers, provide only overall grip strength [13] but fail to distinguish the contribution of individual fingers during specific grasp types. These instruments typically exclude the thumb from measurement, despite its crucial role in grasp stability and overall hand function [14]. As a result, clinicians lack detailed insight into finger-force distribution and coordination patterns, which are essential for evaluating motor recovery and guiding personalized therapy.

Research devices capable of measuring individual finger forces do exist, but they are often technically complex, difficult to operate, or restricted to a single grasp configuration [15], [16]. Moreover, most systems are not modular or compatible with larger experimental setups such as the Shoulder–Elbow Perturbation (SEP) described by Van der Velden et al. (2022) [17], limiting their applicability in both laboratory and clinical environments.

A broader range of sensor-equipped or robotic devices has been developed to assess hand function through kinematic, kinetic, or electrophysiological measurements [18], [19]. Kinematic systems quantify joint angles and range of motion, kinetic systems capture fingertip or grip forces, and electrophysiological systems analyze muscle activation via electromyography (EMG). While valuable, these approaches are generally non-modular, complex, or unsuitable for capturing independent finger forces across predefined grasp types.

To address these limitations, there is a clear need for a compact, modular and clinically practical system that can accurately capture individual finger forces, including the thumb, across multiple functional grasp configurations and in both a standalone and integrated experimental contexts.

C. Objective and scope

The goal of this thesis is to design and validate a modular measurement device capable of quantifying individual finger forces during predefined grasp types. Fig. 1 shows the prototype developed in this project. The device is intended to be operable in the future by post-stroke patients and suitable for both standalone use and integration with external perturbation systems such as the SEP.

This project focuses on the design and prototyping of a complete measurement system consisting of mechanical, electrical, and software subsystems. The development follows an iterative design thinking approach, combining mechanical prototyping and performance testing. The evaluation consists of two phases: a calibration phase, used to verify the accuracy and functionality of the measurement system, and a healthy participant trial phase, used to assess repeatability and ergonomic aspects of the device under realistic operating conditions.

Although the long-term aim of this system is to support post-stroke hand assessment, the present thesis evaluates the device only in healthy participants. Clinical validation and direct patient testing are therefore beyond the scope of this work but are considered important directions for future development once the system's technical feasibility has been demonstrated.

II. Design

A. Method

The development of a force-measurement system for post-stroke patients followed an Iterative Design Thinking approach [20]. This methodology provides a flexible yet systematic framework for creating functional and user-oriented solutions. It consists of six phases: Empathize, Define, Ideate, Prototype, Test, and Implement (Fig. 2). The iterative nature of the process allows transitions back to earlier stages whenever new insights arise, ensuring continuous improvement based on user needs and design feedback throughout the entire development.

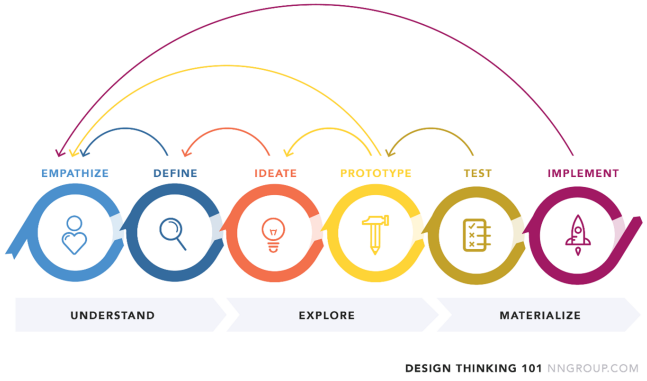

Fig. 2: Iterative Design Thinking process [20].

B. First Design Cycle

The first design cycle aimed to translate initial user needs and technical requirements into a functional proof of concept. The design goal was to create a modular system capable of quantifying hand forces during passive and active movements at different speeds and resistance levels, while also supporting both stand-alone use and integration with perturbation systems.

During the *Empathize* and *Define* phases, the needs of post-stroke patients, researchers, and physical therapists were

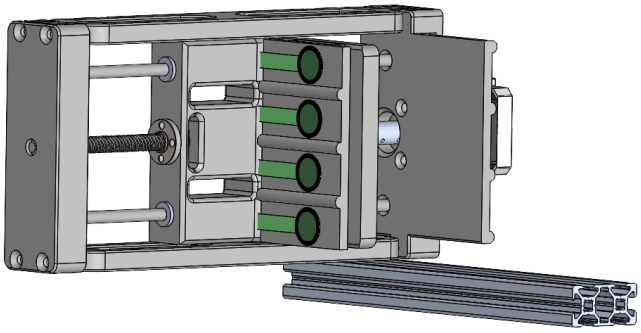

(a) First Prototype Left side

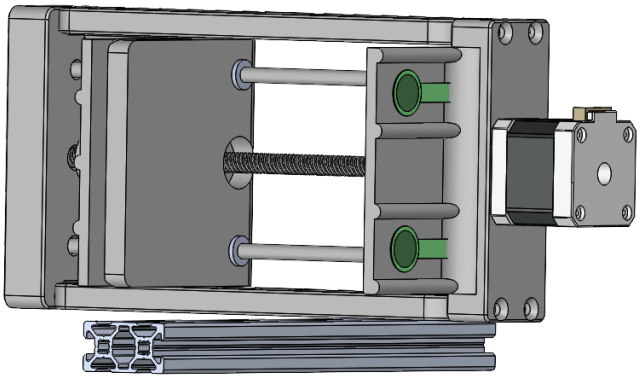

(b) First Prototype Right side

Fig. 3: First prototype developed during the initial design cycle.

identified through literature review and analysis of prior experimental setups. These insights were translated into measurable design requirements (Appendix A). Using these requirements, the *Ideate* phase explored multiple sensing and actuation strategies through a morphological chart (Appendix B). Five concepts were developed and evaluated using a weighted decision matrix based on criteria such as safety, measurement accuracy, actuation performance, ergonomics, and modularity (Appendix C). The Pressure-Slab Mechanism achieved the highest score due to its adaptable geometry and simple actuation strategy.

A CAD prototype was constructed to assess feasibility (Fig. 3). However, critical evaluation revealed key drawbacks. The system was estimated to weigh at least 950 g, making it impractical for attachment to perturbation devices. Furthermore, because the fingers contacted the pressure slabs at an oblique angle, the resulting forces were not purely normal but also contained shear components, which the selected sensors could not detect. These issues indicated that the system's mass and sensing limitations conflicted with its integration and measurement goals, prompting the need for a second design iteration.

C. Second Design Cycle

Evaluation of the first prototype highlighted the need for a simpler, lighter, and passive system capable of accurate finger-force measurement across predefined grasp types. These insights prompted a return to the Empathize phase to refine user needs and system goals.

1) Empathize: The second cycle concentrated on identifying grasps most relevant to post-stroke rehabilitation and bimanual activities of daily living. Stroke patients often use the affected hand primarily for stabilization, making cooperative and support-oriented grasps particularly important [21]. Vergara et al. [22] identified several frequently used grasp types, including the medium wrap, precision disk, lateral pinch, tripod, and lateral tripod (Appendix D).

Based on clinical relevance and feasibility, the medium wrap grasp was selected as the primary target for the next design iteration, with extensions to the precision disk and lateral tripod grasps. These grasps represent a broad and functional range of hand postures suitable for post-stroke assessment.

2) Define: The updated requirements (TABLE I) reflect the shift toward a passive finger-force–measurement device. The refined design goal was to create a modular system capable of measuring individual finger forces during predefined grasps, while remaining lightweight, easily to mount on a 20×40 mm aluminium profile, and operable with minimal setup. Active actuation was removed, but all functional, ergonomic, and safety constraints were retained.

3) Ideate: To accurately measure individual finger forces while maintaining natural motion, a piston-based design was selected in which each finger is mechanically coupled to its own load cell. The pistons provide 6 mm of compliant travel, creating a natural-feeling interface that improves comfort while avoiding excessive movement constraints.

To support multiple grasp types, the device was designed as a modular platform with interchangeable thumb attachments: one positioned laterally for the medium wrap grasp, and another positioned below the finger plane for precision disk or thumb–two-finger grasps. This architecture enabled rapid configuration changes without mechanical redesign.

The resulting conceptual model is shown in Fig. 4 and served as the foundation for further prototyping and refinement.

TABLE I: Updated overview of user, researcher, and therapist requirements.

No.	Requirement	Actor
1	Device should be suitable for the anthropometry of 90% of the adult population (5th–95th percentile).	User
2	Device must be safe during use.	User
3	Device should not constrain finger movement and must allow predefined grasps.	User
4	Device should be made of skin-friendly materials.	User
5	Device should have a high temporal resolution ($\geq$75 Hz).	Researcher
6	Device should support a functional range of motion.	Researcher
7	Device should be modular for easy repair and adjustment.	Researcher
8	Device must be able to measure grip force accurately.	Researcher
9	Device must be mountable on a 20×40 mm aluminium profile.	Researcher
10	Doffing and donning of the device should be possible within 5 minutes.	therapist
11	Device must output measurable data such as force (N).	Therapist

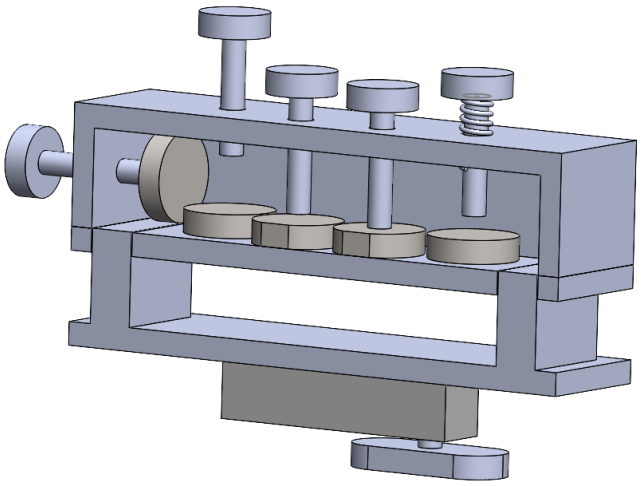

Fig. 4: First Design of the new Concept

III. Final Design

A. Design overview

The prototype phase marked the transition from conceptual design to physical realization. Building on the outcomes of the second design cycle, the final design consists of a modular force-measurement system developed to assess individual finger forces during predefined grasp types in post-stroke patients. The device functions as a stand-alone measurement module but can also be integrated into external perturbation setups such as the SEP. This integration is enabled through its standardized 20×40 mm aluminium profile interface, which provides mechanical compatibility and mounting flexibility across different research environments.

Each finger module incorporates a compact piston mechanism coupled to a digital load cell (FX29, TE Connectivity), allowing precise compression-force measurement along the natural flexion axis of each finger. The design accommodates multiple grasp configurations through two interchangeable thumb modules: one mounted laterally for the medium-wrap grasp, and one positioned beneath the device for the precision-disk grasp. The system can also be configured without any thumb module to enable power-grip measurements. Both thumb modules are reversible, allowing the same hardware to be used for either left- or right-hand assessments.

The final prototype measures 113.5×50×53 mm (L×W×H) without thumb modules. With the lateral thumb attachment, the total length increases to 132 mm, and with the lower thumb module, the total height becomes 88.5 mm (both dimensions including unpressed pistons). The main frame weighs approximately 180 g, and each thumb module adds around 30 g. A detailed overview of all external dimensions is provided in Appendix E, where the full dimensioned drawing of the final device is presented.

The resulting device is compact, lightweight, and ergonomically optimized, providing accurate and repeatable force measurement while remaining intuitive to operate. Its modular architecture and standardized mounting interface make the system suitable for both clinical rehabilitation studies and controlled laboratory experiments.

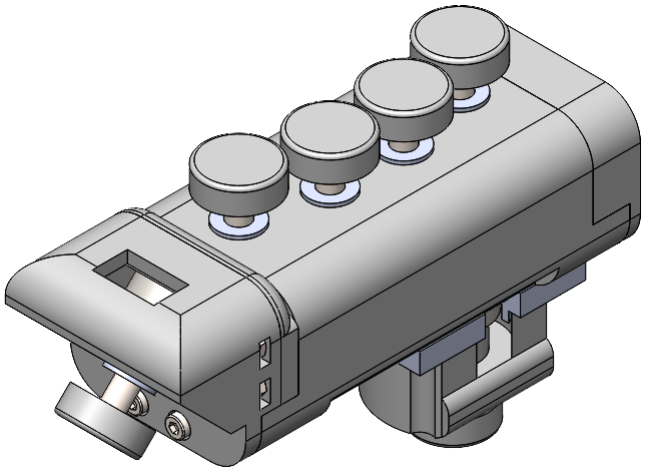

Fig. 5: Isometric CAD view of the modular finger-force measurement device with interchangeable thumb attachments.

B. Mechanical design

The mechanical design aims to achieve precise, low-friction force transmission, robust alignment, and modularity. The device comprises a 3D-printed structural frame that supports four finger modules and one thumb module, as shown in Fig. 5. Each finger module contains:

- a steel piston guided by two plain bearings,
- a compression spring that provides compliant travel and reduces mechanical play,
- a 20 mm circular fingertip pad attached to the piston, and
- a digital FX29 load cell for measuring compressive force.

All custom structural parts were manufactured using fused deposition modeling (FDM) on a Bambu Lab 3D printer with PLA filament, printed by the Faculty Workshop of the Department of Mechanical Engineering at TU Delft. The printed components include the outer frame, sensor housings, spring holders, thumb modules, and fingertip pads.

The pistons are made from M6×40 mm (DIN 912) steel bolts, which were shortened to 15.5 mm. This modification leaves a small threaded section used to attach the circular fingertip pads, while the non-threaded section slides through the plain bearings to ensure smooth linear motion. The use of steel provides high stiffness, wear resistance, and low friction against the bearing surfaces, resulting in accurate and repeatable piston movement.

A sectional view of a single finger module is presented in Fig. 6. The piston shaft slides through an Igus GFM-0608-10 plain bearing (6 mm bore, 8 mm outer diameter), while the 10 mm bolt head is guided within a polyamide plain bearing (IP Sanders 56806.100001, 10×13×15 mm). This dual-bearing configuration provides stable, low-friction guidance and minimizes lateral play during operation.

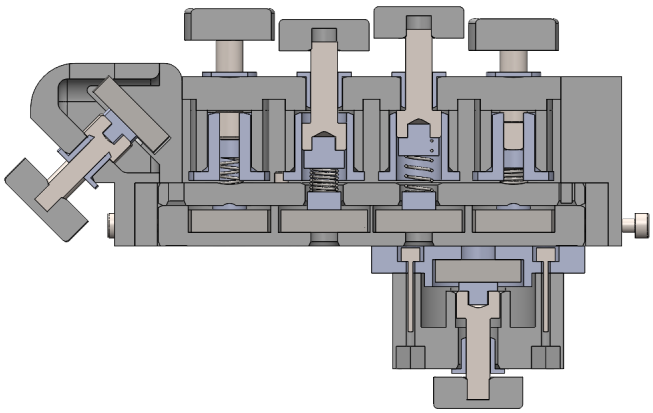

Fig. 6: Sectional CAD view illustrating the concentric alignment of the piston shaft, plain bearings, compression spring, and load cell.

Inside each piston, a 3D-printed PLA insert closes the internal cavity and provides a flat connection surface for the compression spring. A TEVEMA D21500 compression spring is positioned concentrically between the piston insert and the spring holder connected to the load cell. The spring has a free length of 17 mm and generates approximately 10.2 N at 5.9 mm compression. This configuration introduces a small preload that reduces mechanical play and ensures that the sensor remains under a minimal constant load, improving repeatability and tactile comfort.

The selected spring stiffness allows the device to resolve relatively low finger forces, which is particularly important for post-stroke patients who may have substantially reduced strength. At the same time, the 6 mm compliant travel provides a more natural grasping sensation than rigid dynamometer handles, which typically show negligible displacement under load.

The thumb modules use the same FX29 load cells but, due to geometric and spatial constraints, do not incorporate compression springs. Two configurations were designed:

- **Bottom-mounted thumb module (precision disk):** This module is mounted directly beneath the main frame and can be placed on either the left or right side. It enables measurement of a precision-disk grip involving the thumb and the index and middle fingers. The required thumb–finger aperture is approximately 85 mm, which may be challenging for severely impaired post-stroke patients. For this reason, this module is considered optional and intended for participants with sufficient range of motion.
- **Lateral thumb module (medium wrap):** This module is mounted laterally to the frame at a 45° angle, aligning the thumb with a more natural posture during the medium-wrap grasp. Similar to the bottom module, the thumb piston is directly coupled to the load cell without a spring.

In both thumb modules, the piston follows the same basic design as the finger pistons (shortened M6×40 mm bolt with a PLA insert), but uses a single 6 mm bearing for guidance due to the reduced available space and the load cells are not preloaded in these configurations.

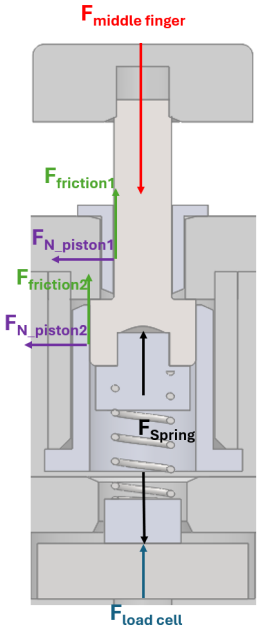

Fig. 7: Simplified free-body diagram of a single finger module, showing the main load path through the piston–spring–sensor assembly.

Together, the frame, finger modules, and thumb modules form a compact and modular mechanical system that supports accurate and repeatable finger-force measurements across multiple grasp configurations.

C. Force transfer and measurement principle

The force applied by the finger on the fingertip pad is transmitted through the steel piston and compression spring to the FX29 digital load cell mounted beneath each module. The load cell converts the compressive force into a digital signal proportional to the applied finger force. The bearing-guided piston constrains motion to a single translational degree of freedom, so that the sensor is predominantly loaded in axial compression.

A simplified free-body diagram of a single finger module is shown in Fig. 7. The applied finger force F_{Finger} acts approximately vertically downward on the piston, which compresses the spring and transmits the load to the sensor. The spring force is given by

$$F_{\text{Spring}} = k\,u,$$

where k is the spring stiffness and u is the spring compression. In static equilibrium, the sensor reaction force $F_{\text{Load,cell}}$ equals the axial component of the finger force minus losses due to friction.

Frictional forces in the bearings can be expressed as

$$F_{\text{Friction}} = \mu\,F_{N,\text{piston}},$$

where μ is the friction coefficient and $F_{N,\text{piston}}$ is the normal reaction between the piston and the bearing surfaces. When the applied finger force is not perfectly perpendicular to the fingertip pad, the lateral component of the force increases $F_{N,\text{piston}}$, which in turn increases F_{Friction} and slightly reduces the measured $F_{\text{Load,cell}}$. However, due to the low friction of the lubricated plain bearings and the relatively small finger-force angles used during testing, these effects remain within the specified non-linearity and hysteresis bounds of the sensor.

A more detailed full body diagram of the precision-disk and medium wrap is provided in Appendix F

D. Electronics and sensors

The system uses six TE Connectivity FX29 digital compression load cells (I^2C output, 125 N range) [23]. Each sensor provides a 14-bit digital output over an effective range of approximately 1000–15000 counts, corresponding to a nominal resolution of

$$\frac{125\ \text{N}}{14\,000} \approx 0.0089\ \text{N/count}.$$

According to the datasheet, the sensors exhibit a non-linearity of $\pm 1\%$ and a hysteresis of $\pm 0.8\%$ of full scale, corresponding to approximately ± 1.25 N and ± 1.0 N over the 125 N range. Their small diameter (20 mm) and through-hole mounting make them suitable for compact integration beneath each piston module.

All FX29 load cells share the same I^2C address (0x28). To enable multi-sensor operation, a TCA9548A I^2C multiplexer is used to switch between sensors. Each sensor is connected to a dedicated multiplexer channel, which can be enabled and disabled under software control. The sensors and multiplexer are powered by a regulated 5 V supply, with 4.7 kΩ pull-up resistors on the SDA and SCL lines to ensure reliable communication.

The multiplexer output is connected to an Arduino Uno R3, which serves as the central data acquisition unit and provides the 5 V supply. The Arduino sequentially cycles through the multiplexer channels and reads each sensor at 100 Hz per full six-sensor cycle, resulting in synchronized measurements across all fingers. A complete wiring diagram, including pin assignments and cable routing, is provided in Appendix G.

E. Control and software

The control and data acquisition pipeline is divided between the Arduino Uno firmware and a Python-based graphical user interface (GUI) running on a PC.

On the embedded side, custom Arduino firmware manages:

- sequential polling of all six FX29 sensors via the I^2C multiplexer,
- automatic tare corrections when sensor values remain within a no-load window of ± 50 counts,
- conversion from raw counts to calibrated force values using sensor-specific calibration parameters, and
- serial transmission of time-stamped force data at 250 kbaud.

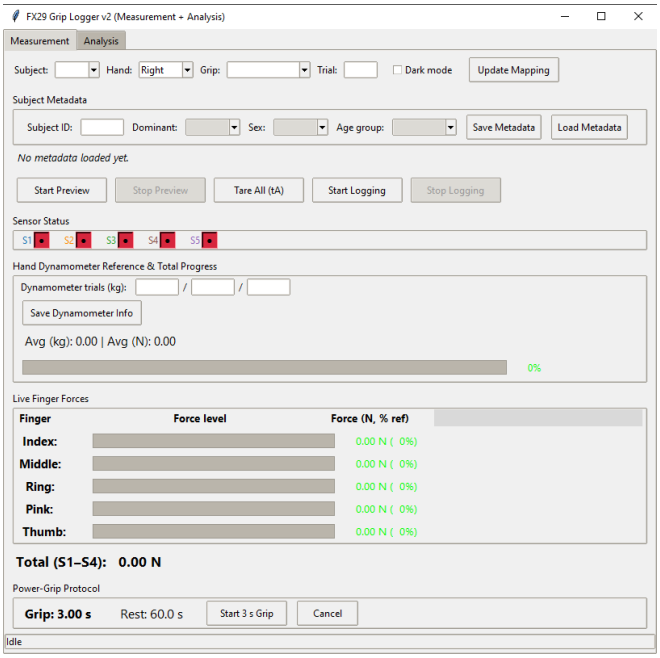

Fig. 8: Python-based graphical user interface used for live visualization and logging of multi-finger force measurements.

The calibration slope and offset for each sensor are stored directly in the Arduino sketch, enabling real-time conversion to newtons without additional post-processing.

On the PC side, a custom Python GUI receives the serial data stream, decodes the per-sensor forces, and visualizes them in real time (Fig. 8). The interface displays:

- individual finger forces,
- the total grip force of the four base fingers,
- the currently selected grasp type and subject ID,
- trial status and basic quality indicators.

Before each measurement, the user can select the grasp type (medium wrap, precision disk, power grasp), subject number, and trial parameters. The GUI also provides a manual tare function to zero all sensors at the start of a session. All raw force data are logged to CSV files for offline analysis.

In addition to numerical readouts, the GUI includes a plotting module that can generate real-time force–time traces for each finger and for the total grip force. These visualizations allow rapid assessment of signal quality, drift, and participant performance. Together, the Arduino firmware and Python GUI form a compact and flexible control system that supports synchronized multi-sensor operation, live feedback, and efficient data management during calibration and experimental trials.

All code used in this project is openly available on GitHub: `https://github.com/jvanaernsberge/GUI-and-arduino-code-for-hand-assessment-device`.

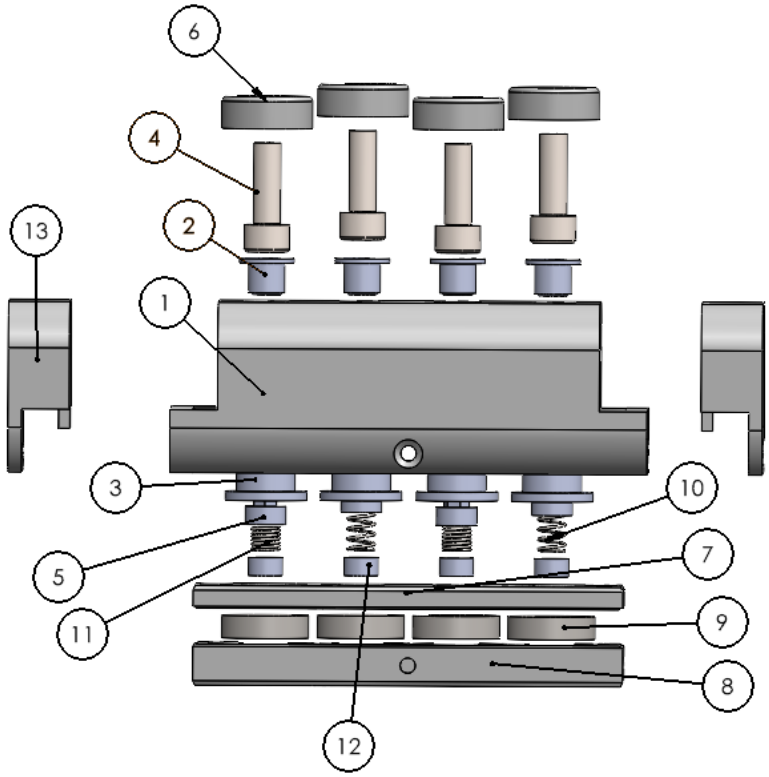

ITEM NO.	PART NUMBER	QTY.
1	Main Frame	1
2	IGUS GFM-06-08-10	6
3	IP Sanders 56806.100001	4
4	DIN 912 M6 x 40 --- 24N	4
5	Piston insert	4
6	Finger contact pad	6
7	Top alignment plate	1
8	Base plate	1
9	FX29K0-100A-0025-L sensors	6
10	D21500 L0	2
11	D21500 Ln	2
12	Load caps	4
13	Side cover	2

Fig. 9: Exploded CAD view of the main finger module.

F. Assembly and integration

The complete device with both thumb configurations is shown in Fig. 5, while Fig. 9 presents an exploded view of the main finger module.

Assembly proceeds as follows:

1) Press-fit the 6 mm and 10 mm plain bearings into the main 3D-printed frame.
2) Insert the lubricated steel pistons through the bearings and attach the fingertip pads.
3) Mount and align the FX29 load cells in the base plate so that the spring holders or piston inserts contact the centre of the sensing surface.
4) Install the compression springs between the piston inserts and the spring holders, introducing a small preload to eliminate mechanical play.
5) Slide the lower subassembly (sensors, springs, and base plate) into the main frame and secure it with screws.
6) Attach the desired thumb module:
   - no-thumb configuration: install both side covers;
   - lateral thumb module (medium wrap): replace one side cover with the lateral thumb assembly at 45°;
   - bottom thumb module (precision disk): mount the bottom module beneath the frame after removing the lower cover section.
7) Connect the sensors and multiplexer according to the wiring scheme and mount the device to a 20×40 mm aluminium profile using the integrated interface.

Each module can be replaced or repositioned independently without disturbing the others. The concentric alignment of piston, spring, and sensor ensures consistent load transmission and repeatable force readings after reassembly. In practice, the system can be reconfigured between grasp types or participants in under ten minutes.

IV. Evaluation

A. Calibration

The calibration establishes the relationship between the raw sensor output and the applied force. Each FX29 load cell was calibrated using a rope-and-weight setup in which known masses were applied through a piston that loaded the sensor directly (Fig. 10). A zero-load reference was first recorded, after which five incremental masses (0 g, 500 g, 990 g, 1490 g, 2043 g) were applied in a stepwise manner. The raw 14-bit output at each step was logged and used to derive the sensor-specific calibration slope (counts/N). All steps were repeated three times to verify stability and linearity. A detailed description of the physical setup and calibration measurements is provided in Appendix H.

B. Live Data Validation

To verify calibration accuracy under continuous loading, each sensor was tested at 100 Hz using the same loading procedure and an additional step of 2533 g to assess interpolation beyond the calibrated range. For each load, the measured force was compared to the known applied mass and

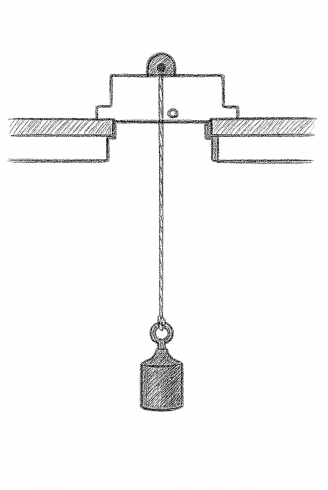

Fig. 10: Sketch of Sensor calibration setup

evaluated in terms of mean and maximum deviation relative to full scale (FS). Across all sensors, errors consistently remained within 0–1 %FS, which aligns with the FX29 accuracy specification and confirms reliable force estimation under both axial and mildly off-axis loading conditions.

C. Low-Load Range Improvement

Initial validation indicated increased variability in the 0–1 kg range, primarily due to friction in the piston–bearing interface at low spring compression and limited calibration density in this region. To address these limitations, three targeted improvements were implemented:
(1) lubrication of the piston assembly to reduce friction and stick–slip,
(2) replacement of the 3D-printed spring holders with laser-cut PMMA for improved alignment, and
(3) a refined calibration protocol incorporating additional low-weight steps (200 g, 250 g, 450 g, 500 g, 700 g, 750 g, and 990 g).

Subsequent re-validation demonstrated a reduction in mean calibration error from 0.21 %FS to 0.10 %FS, representing a 52 % improvement in the low-load region. All sensors remained well within the 1 %FS accuracy specification. The full validation procedure and results are presented in Appendix H.

D. User validation

The objective of the user validation study was to evaluate the device's performance in terms of measurement repeatability, accuracy, and ergonomic comfort. This stage aimed to confirm that the device functions as intended and provides a natural and comfortable fit for the user.

Thirteen healthy adults (4 female, 9 male), aged 18–65 years, participated in the study. All participants provided written informed consent in accordance with the Human Research Ethics Committee (HREC) guidelines (approval number: 6129). The full informed consent form and the participant-information document are included in Appendix J. To avoid inter-hand variability, only the dominant hand was tested (10 right-hand dominant, 3 left-hand dominant). Most participants were young adults (18–25 years: 8 participants), with additional representation from the 26–35 (3 participants), 46–55 (1 participant), and 56–65 (1 participant) age groups. Each testing session lasted approximately 30–45 minutes.

The test consisted of the following:

- **Medium Wrap grip:** The four fingers (index, middle, ring, and little finger) rest on top of the device, with the thumb placed laterally at approximately 45°.
- **Precision Disk grip:** The thumb, index, and middle finger contact the device in a small-object pinch configuration.
- **Power Grasp:** All four fingers wrap around the device while the thumb opposes the fingers.
- **Grip strength with hand dynamometer:** Maximal voluntary contractions (MVCs) were performed for all three grasp types using a commercial hand dynamometer (Inaepeak Electronic Hand Dynamometer) as a validated reference.

Each participant completed one familiarization trial per grasp, followed by three to four recorded trials, as recommended in hand-strength reliability studies [24], [25], [26]. Each trial consisted of a 3 s maximal voluntary contraction, a duration commonly used in grip- and finger-force protocols [27], [28]. To prevent fatigue and preserve maximal force output, a rest period of at least 60 s was provided between trials in accordance with established recovery guidelines [29], [30], [31]. After completing all grasp tasks, participants filled out a short questionnaire on comfort, hand placement, and usability (Appendix K).

Quantitative evaluation: Three complementary metrics were used to quantify measurement repeatability and accuracy.

1) Standard deviation (SD): Repeatability was first assessed using the standard deviation of repeated trials for each subject and grasp.

$$SD = \sqrt{\frac{1}{N-1}\sum_{i=1}^{N}(F_i - \bar{F})^2}. \tag{1}$$

Here, F_i is the maximal force of trial i, $\bar{F}$ is the subject-specific mean force, and N is the number of trials. SD represents the absolute variability between trials. Since human grip force shows inherent biological variation, SD values from the device are expected to be similar to those of the dynamometer.

2) Normalized trial-to-mean deviation: Relative trial precision was evaluated using the normalized deviation from each subject's mean:

$$\delta_i = \frac{|F_i - \bar{F}|}{\bar{F}} \times 100\%. \tag{2}$$

Here, δ_i represents the relative deviation of trial i from the subject-specific mean force $\bar{F}$, expressed as a percentage. Each δ_i therefore corresponds to a single recorded trial. These deviations were visualized using circular scatter plots

with a $\pm 10\%$ threshold, reflecting typical human repeatability limits for maximal grip force. Trials within this 10% band primarily represent normal human variability rather than device noise.

3) Coefficient of variation (CV): The coefficient of variation expresses variability relative to the mean:

$$CV = \frac{SD}{\bar{F}} \times 100\%. \tag{3}$$

CV is widely used in handgrip literature and provides a normalized measure of repeatability. Acceptable values for maximal grip strength are approximately 10% for males and 12% for females [32].

Success criteria: The device is considered validated if:

- The SD values per grasp are similar to those measured with the dynamometer.
- The proportion of trials within the $\pm 10\%$ deviation band matches that of the dynamometer.
- The group-level CV per grasp falls within the expected human variation range (10–12%).

E. User validation results

The user validation resulted in a total of 146 valid trials. TABLE II summarizes the number of valid trials per grasp and subject. Depending on the grasp configuration and measurement quality, participants contributed between nine and twelve valid trials in total.

Classification of invalid trials: Before analysis, all recorded trials were screened for validity. A trial was classified as invalid and excluded when one or more of the following conditions occurred:

- **Grasp or positioning inconsistency:** deviations in how the hand, wrist, thumb, or fingers were positioned within the intended grasp (e.g., shifted palm contact, altered thumb height, or changed finger alignment on the pistons), resulting in atypical or non-representative force values.
- **Participant-related limitations:** discomfort or momentary interruption preventing a full and representative maximal effort.
- **Sensor issues:** missing or incomplete force readings, such as a non-recording thumb sensor or measurement dropout.

TABLE II: Number of valid trials per grasp type and subject.

Subject	MediumWrap	PrecisionDisk	Power Grasp	Total
1	3	3	3	9
2	3	4	3	10
3	3	4	4	11
4	3	3	4	10
5	4	4	4	12
6	4	4	4	12
7	4	4	4	12
8	4	4	4	12
9	3	4	4	11
10	4	4	3	11
11	4	4	4	12
12	4	4	4	12
13	4	4	4	12
Total	**47**	**50**	**49**	**146**

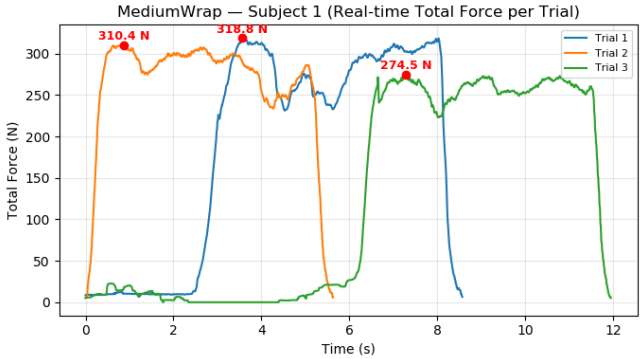

Fig. 11: Example of total force (summed across active sensors) for a Medium Wrap trial. Peak values, which are marked with red points, were used to compute the per-subject mean and SD.

Only trials that consistently reflected the intended grasp type, proper hand placement, and valid sensor output were retained for further analysis. These valid trials were then used to evaluate the device's measurement accuracy and repeatability across all grasp types. Analyses were performed at both the individual level (repeatability within subjects) and the group level (variability between subjects), providing a comprehensive assessment of system performance.

1) Subject-level precision: For each trial, the total force at peak contraction (sum of active fingers) was computed, following the same procedure used by commercial dynamometers. An example is shown in Fig. 11. Averaging SD values across all subjects yields:

- Medium Wrap: 19.1 N (dynamometer) vs. 20.8 N (device)
- Precision Disk: 3.6 N (dynamometer) vs. 9.2 N (device)
- Power Grasp: 17.3 N (dynamometer) vs. 13.8 N (device)

Overall, the device matches the dynamometer closely, and the remaining variation is dominated by normal biological differences between trials. A complete set of per-subject SD plots for all grasp types is provided in Appendix I.

2) Group-level precision: Fig. 12 shows the distribution of normalized deviations for all trials. The device and dynamometer demonstrate nearly identical repeatability:

- Device: 84.9% of trials within $\pm 10\%$; 59.6% within $\pm 5\%$
- Dynamometer: 85.5% within $\pm 10\%$; 62.4% within $\pm 5\%$

Group-level CV values also fall comfortably within physiological limits:

- Medium Wrap: 9.45%
- Precision Disk: 4.62%
- Power Grasp: 7.30%

3) Finger-force distribution: Finally, the device's finger-force distributions at peak force were compared with published reference studies (TABLE III). For all three grasp types, the prototype aligns closely with literature values. For cylindrical grasping increasing handle diameter reduces the

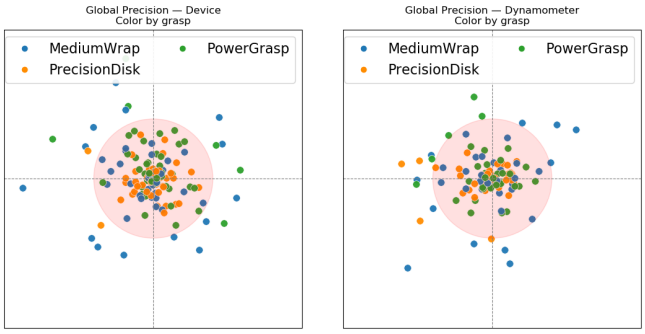

(a) Device (b) Dynamometer

Fig. 12: Polar scatter plots of normalized trial-to-mean deviations (δ_i) for all subjects and grasp types. Each point shows a trial's deviation from that subject's mean peak force. The radial axis denotes δ_i (in %), where smaller radii indicate higher repeatability. Colours represent grasp types (Medium Wrap, Precision Disk, Power Grasp), and the shaded ring indicates the $\pm 10\%$ band commonly reported as the natural repeatability limit for maximal grip-force tasks. Both the prototype device and dynamometer show similar distributions, with most trials falling within this physiological range.

dominance of the index finger and produces a more uniform distribution of forces, a trend confirmed in the present data [33].

Finally, the device's finger-force distributions at peak force were quantified for all three grasp types. The measured contributions per finger followed clear and grasp-specific patterns, with the middle finger providing the largest share during the Power Grasp and the thumb dominating the Precision Disk. Corresponding plots and data of these distributions are provided in Appendix L.

4) Questionnaire feedback: All thirteen participants completed the ergonomic questionnaire included in Appendix K. The questionnaire covers hand placement, comfort, grasp experience, mechanical behavior, and overall usability. The results of each section are summarized below.

Hand placement and fit. A total of 11 out of 13 participants stated that hand placement felt natural and aligned well with their grasp posture (scores 4–5). One participant (P5) indicated that the device was too large for their hand, which was confirmed across multiple items in their responses. All remaining participants reported that the device accommodated their hand size comfortably. These findings suggest that the current dimensions are suitable for most users, but that a smaller or adjustable variant would improve usability for individuals with smaller hands.

Ergonomic comfort. During maximum squeezing, 11 out of 13 participants reported feeling comfortable. Two participants noted that the finger contact pads had sharp edges that pressed uncomfortably against the distal interphalangeal (DIP) joint. Furthermore, 7 out of 13 participants reported that the bottom plate felt sharp during the power grasp, due to the thumb pressing against the lower edge. These comments consistently identify insufficiently rounded edges as the primary comfort-related limitation of the prototype.

Grasp experience. The Medium Wrap was rated as the most comfortable grasp by 8 out of 13 participants, whereas the Precision Disk was rated as the least comfortable by 8 out of 13 participants. The Precision Disk was mainly criticized for feeling unnatural when producing maximal force using only three fingers. Five of the eight participants who rated it lowest explicitly mentioned this unnatural finger posture. The Power Grasp received lower comfort scores primarily due to the sharp bottom-plate edge, which became more noticeable during high-force contractions.

Mechanical behavior. A clear majority of participants (12 out of 13) reported no noticeable mechanical resistance, friction, or misalignment. The pistons were consistently described as smooth and responsive. Only one participant (P1) noticed a "clicking" sensation at the end of piston travel, which was resolved before subsequent testing. Overall, the mechanical performance of the device was rated very positively.

General impression. Most participants found the device intuitive and ergonomic, with 8 out of 13 providing a score of 4 or higher. Nine participants stated that the prototype felt more comfortable and less slippery than the hand dynamometer. The most frequently suggested improvements concerned removing sharp edges on the base plate, rounding the contact surfaces, and adding a softer material layer to the finger pads instead of relying solely on the hard 3D-printed surface.

The following recurring themes were identified across all participants:

- **Sharp edges:** Reported by 7 participants as the most prominent ergonomic issue.
- **Precision grasp discomfort:** Mentioned by 8 participants, indicating a clear need for redesign of this configuration.
- **Medium Wrap comfort:** Identified as the most comfortable grasp by 8 participants.
- **Prototype vs. dynamometer:** Nine participants preferred the prototype, noting improved comfort and reduced slipperiness.
- **Mechanical stability:** Twelve participants reported no issues with friction, misalignment, or finger-pad motion.
- **Size mismatch:** Two participants with smaller hands found the device slightly too large.

TABLE III: Finger force distribution (%) per grasp type, including literature references.

Medium Wrap	**Index**	**Middle**	**Ring**	**Pink**	**Thumb**
Prototype	17.6	22.8	18.8	10.3	30.5
[34]	18.0	23.0	17.0	11.0	31.0
Power Grasp	**Index**	**Middle**	**Ring**	**Pink**	**Thumb**
Prototype	23.4	34.6	27.4	14.6	–
[35]	24.7	35.7	28.3	11.3	–
[36]	30.0	30.0	22.0	18.0	–
[33]	20.6	38.9	26.9	13.6	–
Precision Disk	**Index**	**Middle**	–	–	**Thumb**
Prototype	25.4	26.2	–	–	48.4
[37]	28–30	23–28	–	–	45–48

- **Wrist posture:** Three participants experienced an unnatural wrist position for specific grasps.
- **Button geometry:** Four participants found the buttons too sharp or flat and suggested rounding them.
- **Surface texture:** Two participants recommended a textured or softer surface, especially for precision and power grasps.

V. Discussion

A. Hand function assessment device prototype

The device developed in this study aimed to provide a modular, compact system capable of measuring individual finger forces, including the thumb, across multiple functional grasps. This objective addresses the limitations of existing devices, which typically either fail to distinguish finger-specific contributions, exclude the thumb, support only a single grasp configuration, or rely on complex, non-modular setups that cannot be easily integrated with perturbation systems.

The design emphasizes simplicity and rapid module exchange, supporting efficient clinical assessment of hand function. However, measurement stability is highly sensitive to the mechanical alignment between pistons, guide surfaces, and sensors. The chosen modular architecture introduces trade-offs between compactness, structural stiffness, and alignment tolerance, which influenced several key design choices. The overall module size is further constrained by component dimensions: the FX29 sensor (20 mm diameter) sets a lower bound on housing width, while the selected spring stiffness and displacement path, required to provide a natural grasping feel, add additional volume. Together, these factors limit how compact the device can be. Small deviations arising from 3D-printed manufacturing tolerances, clearance between pistons and bearings, friction at the load interface, or intrinsic sensor variability can collectively introduce measurable errors in the recorded forces.

B. Validation

Calibration showed that all sensors operated well within their specified accuracy range. The mean error was 0.12% FS ($\approx$ 0.125 N) and the maximum error 0.55% FS ($\approx$ 0.69 N), corresponding to a worst-case measurement error of approximately 2.2% for the lowest observed peak force (31 N, Precision Disk). Sensor drift remained minimal across trials but became noticeable at very low forces (< 2 N), where the FX29 approaches its noise floor and mechanical tolerances introduce proportionally larger fluctuations. This limits the device's suitability for fine-force control measurements but does not affect maximal grasp-force assessments.

Participant validation demonstrated high repeatability for all grasp types. SD, CV, and normalized precision metrics were comparable to those of a commercial dynamometer, indicating that most variability originates from biomechanical factors rather than measurement noise. The MediumWrap showed the lowest repeatability, which is consistent with its greater biomechanical degrees of freedom and the involvement of more digits. This pattern matches expectations for cylindrical grasps and confirms that variability in these trials primarily reflects grasp mechanics.

The device also reproduced the characteristic finger-force distribution patterns reported in the literature. For the Medium Wrap, all five digits were within approximately 0–2 percentage points of reference values. Power Grasp distributions showed slightly larger deviations: the device differed by 1–3 percentage points compared with Li et al. and Seo et al., and by up to 4–7 percentage points relative to Kinoshita's earlier measurements, which report a different distribution pattern. For the Precision Disk, deviations across the thumb and index–middle pair typically fell within 1–4 percentage points of the published ranges. These error margins follow expected distinctions between cylindrical grips, which produce flatter multi-finger distributions, and pinch-like grasps, which are dominated by the thumb. Together, these findings support the construct validity of the measurement system.

Ergonomically, participants reported that the device offered a stable and natural grasping sensation and was less slippery than the commercial dynamometer. Most subjects preferred the prototype during maximal-force tasks, although several noted discomfort due to sharp geometric transitions on the base plate and contact surfaces. These observations highlight that the ergonomic experience is promising but requires targeted refinement for clinical use.

Overall, the validation results demonstrate that the prototype achieves its intended performance goals in terms of accuracy, stability, and repeatability for the tested grasp types. However, the present evaluation was performed exclusively in healthy adults. Although the device was specifically designed with post-stroke hand assessment in mind, it has not yet been evaluated in this population. Testing with post-stroke participants remains a crucial next step to determine its clinical viability, accessibility, and usability in impaired hands.

C. Limitations

The device relies on precise mechanical alignment between pistons, bearings, and sensors. Small deviations caused by 3D-printed tolerances, clearance in the piston–bearing interface, or friction at the load surface introduce measurable variability and occasional piston tilting. These effects were not fully optimized due to prototyping constraints and would require higher-precision manufacturing for clinical-grade accuracy.

Most structural components were fabricated from PLA, which is prone to wear, creep, and dimensional drift under repeated loading. As a result, long-term mechanical stability and calibration retention were not evaluated and cannot be guaranteed without material or manufacturing upgrades.

The FX29 sensors show reduced accuracy at low forces (< 2 N), limiting their suitability for fine-force control tasks. At the upper end of the sensing range (125 N), the thumb approached sensor saturation in several trials, and one subject reached this limit. While unlikely in post-stroke populations,

this may constrain measurements in healthy subjects or during perturbation-based experiments.

Wrist posture was not constrained during the trials, allowing drift in hand position within and between subjects. Although participants were instructed to maintain a consistent posture, variation in wrist angle and finger alignment likely contributed to variability, particularly in the MediumWrap grasp. Grasp posture was not recorded using motion tracking or imaging, leaving the extent of posture-related variability unquantified. These findings also relate to the variability differences observed across grasp types, with MediumWrap showing the lowest repeatability in the evaluation, driven largely by biomechanical freedom rather than device limitations.

Direct accuracy validation was limited. The dynamometer served as a reference, but differences in handle geometry (notably a thinner grip) resulted in higher maximal forces on the dynamometer than on the device for MediumWrap and PowerGrasp. Only PrecisionDisk forces were comparable, complicating absolute accuracy comparison. Nevertheless, because the device consistently reproduced internal distribution patterns and matched the dynamometers repeatability metrics, the measurement accuracy can be considered sufficient for relative-force assessment across fingers and grasps, even though absolute maximum-force comparability remains grip-geometry dependent.

The lower thumb module requires a large hand aperture due to integrated mechanical components, which may pose challenges for individuals with reduced hand opening. Sharp geometric transitions and hard contact surfaces may also influence comfort during maximal squeezing.

Several study-design constraints limit generalization. The sample size was small (13), and participants were predominantly young adults (18–25 years). Only dominant hands were tested, which may underestimate variability present in non-dominant or impaired hands. Fatigue was not assessed, despite repeated maximal contractions that may influence later trials.

Finally, the device was tested exclusively under static maximal-force conditions. Dynamic or time-varying force tracking was not evaluated. Although the system was designed for SEP integration, perturbation-induced effects, such as vibration, alignment shifts, or dynamic loading, were not assessed. A dedicated mounting module for a 20x40 aluminium profile was produced, but not experimentally validated.

D. Future work and recommendations

Future improvements should prioritize higher-precision manufacturing of the pistons, bearings, and guides to minimize tilting and friction, and the use of higher-quality yet lightweight materials to improve durability and calibration stability. In addition, future healthy-participant testing should be performed under constrained wrist posture to reduce posture-related variability and better isolate the mechanical behavior of the device. Trials with post-stroke participants are essential to assess usability, grasp feasibility, accessibility of the grasp aperture, and the device's ability to detect impaired finger coordination and altered force-sharing strategies. Multi-day testing should also be conducted to establish ICC(2,1) test–retest reliability and to examine how calibration stability evolves over longer periods of use.

Integration with the SEP represents the next major development stage. The device should be tested under perturbation to evaluate how vibration, rapid arm motion, and dynamic loading influence force measurements, mechanical alignment, and user control. The lower thumb module also requires redesign to reduce the required hand aperture, thereby improving accessibility for users with limited range of motion and better accommodating post-stroke hand-opening constraints.

Several design refinements can further enhance ergonomics and usability. The piston contact surfaces would benefit from defined finger-placement features, such as shallow grooves, to improve consistency of finger positioning. A softer surface coating could increase comfort during maximal squeezing. The base plate should incorporate rounded edges, particularly near the cable exit, or be fully enclosed to eliminate sharp transitions. Lateral cable routing that does not interfere with modularity would improve ease of use, and a soft, non-interfering bottom surface may reduce discomfort when the device is pressed against the palm during forceful grips.

E. Clinical Relevance

The device enables the quantification of individual finger forces and their distribution across multiple grasp types, providing clinically valuable insight into finger coordination patterns that cannot be captured with traditional dynamometers. Its modular design allows clinicians to assess grasp-specific impairments and compare functional patterns across different tasks. Because the system measures both strength and force control, it supports evaluation of multiple dimensions of hand function. Additionally, the device may help identify compensatory strategies, such as over reliance on stronger fingers or reduced thumb contribution, that are relevant for diagnosis and personalized therapy planning. In addition, the strong user preference for the prototype over the dynamometer indicates that the device may better support naturalistic hand placement and consistent maximal-effort execution, which is beneficial for repeated clinical measurements.

VI. Conclusion

In this study, a modular hand-function assessment device was developed to quantify individual finger forces, including the thumb, across multiple functional grasp types. The design integrates five FX29 load cells in interchangeable grasp modules. The system emphasizes simplicity, compactness, and rapid module exchange, making it suitable for both laboratory experiments and future clinical use.

Calibration and healthy-participant testing demonstrated that the device performs reliable within its intended operating

range. Sensor accuracy remained within specification, and drift was minimal except at very low forces. Participant trials showed high repeatability for all grasps, with performance comparable to a commercial dynamometer. The device also reproduced expected biomechanical force-distribution patterns, confirming that it captures meaningful aspects of finger coordination.

All in all, the device shows strong potential as a practical, modular tool for detailed assessment of hand function in both research and rehabilitation contexts.

VII. Acknowledgment

The author wishes to express sincere gratitude to Dr. ir. Arno H. Stienen for his supervision, guidance, and valuable feedback throughout this thesis, and to ir. J.C. van Zanten for his daily supervision, guidance and valuable feedback. The author also thanks J.A. Brenkman for his assistance with sensor wiring, including soldering, connector preparation, and practical advice on the electrical integration. Appreciation is extended to the participants whose voluntary and uncompensated involvement were essential for the experiments.

Acknowledgment is also given to the use of ChatGPT-4 (OpenAI) for assistance in refining grammar and clarity in the written text, and for support in debugging and structuring elements of the Arduino firmware and Python-based GUI. All content produced with its assistance was critically reviewed, edited, and validated by the author to ensure accuracy, originality, and compliance with academic and ethical standards.

References

[1] V. L. Feigin, M. Brainin, B. Norrving, S. O. Martins, J. Pandian, P. Lindsay, F. G. M, and I. Rautalin, "World stroke organization: Global stroke fact sheet 2025," *Int J Stroke*, vol. 20, no. 2, pp. 132–144, 2025.

[2] P. Raghavan, "Upper limb motor impairment after stroke," *Phys Med Rehabil Clin N Am*, vol. 26, no. 4, pp. 599–610, 2015.

[3] J. Plantin, G. V. Pennati, P. Roca, J. C. Baron, E. Laurencikas, K. Weber, A. K. Godbolt, J. Borg, and P. G. Lindberg, "Quantitative assessment of hand spasticity after stroke: Imaging correlates and impact on motor recovery," *Front Neurol*, vol. 10, p. 836, 2019.

[4] C. Trompetto, L. Marinelli, L. Mori, E. Pelosin, A. Currà, L. Molfetta, and G. Abbruzzese, "Pathophysiology of Spasticity: Implications for Neurorehabilitation," *BioMed Research International*, vol. 2014, pp. 1–8, 1 2014. [Online]. Available: https://pmc.ncbi.nlm.nih.gov/articles/PMC4229996/

[5] K. Sakuma, K. Ohata, K. Izumi, Y. Shiotsuka, T. Yasui, S. Ibuki, and N. Ichihashi, "Relation between abnormal synergy and gait in patients after stroke," *Journal of NeuroEngineering and Rehabilitation*, vol. 11, no. 1, p. 141, 1 2014. [Online]. Available: https://doi.org/10.1186/1743-0003-11-141

[6] M. Alt Murphy, C. Willen, and K. S. Sunnerhagen, "Movement kinematics during a drinking task are associated with the activity capacity level after stroke," *Neurorehabil Neural Repair*, vol. 26, no. 9, pp. 1106–15, 2012.

[7] N. Kang and J. H. Cauraugh, "Force control in chronic stroke," *Neurosci Biobehav Rev*, vol. 52, pp. 38–48, 2015.

[8] S. M. Lai, S. Studenski, P. W. Duncan, and S. Perera, "Persisting consequences of stroke measured by the stroke impact scale," *Stroke*, vol. 33, no. 7, pp. 1840–4, 2002.

[9] V. M. Parker, D. T. Wade, and R. Langton Hewer, "Loss of arm function after stroke: measurement, frequency, and recovery," *Int Rehabil Med*, vol. 8, no. 2, pp. 69–73, 1986.

[10] K. D. Rech, A. P. Salazar, R. R. Marchese, G. Schifino, V. Cimolin, and A. S. Pagnussat, "Fugl-meyer assessment scores are related with kinematic measures in people with chronic hemiparesis after stroke," *J Stroke Cerebrovasc Dis*, vol. 29, no. 1, p. 104463, 2020.

[11] K. Marek, J. Redlicka, E. Miller, and I. Zubrycki, "Objectivizing measures of post-stroke hand rehabilitation through multi-disciplinary scales," *J Clin Med*, vol. 12, no. 23, 2023.

[12] E. T. Wolbrecht, J. B. Rowe, V. Chan, M. L. Ingemanson, S. C. Cramer, and D. J. Reinkensmeyer, "Finger strength, individuation, and their interaction: Relationship to hand function and corticospinal tract injury after stroke," *Clinical Neurophysiology*, vol. 129, no. 4, pp. 797–808, 2018.

[13] A. Sunderland, D. Tinson, L. Bradley, and R. L. Hewer, "Arm function after stroke. an evaluation of grip strength as a measure of recovery and a prognostic indicator," *J Neurol Neurosurg Psychiatry*, vol. 52, no. 11, pp. 1267–72, 1989.

[14] G. Cotugno, K. Althoefer, and T. Nanayakkara, "The role of the thumb: Study of finger motion in grasping and reachability space in human and robotic hands," *IEEE Transactions on Systems, Man, and Cybernetics: Systems*, vol. 47, pp. 1–10, 04 2016.

[15] G. Kurillo, M. Mihelj, M. Munih, and T. Bajd, "Multi-fingered grasping and manipulation in virtual environments using an isometric finger device," *Presence: Teleoperators and Virtual Environments*, vol. 16, no. 3, pp. 293–306, 2007.

[16] A. Chen, K. Lee, L. Winterbottom, J. Xu, C. Lee, G. Munger, A. Deli-Ivanov, D. M. Nilsen, J. Stein, and M. Ciocarlie, "Volitional control of the paretic hand post-stroke increases finger stiffness and resistance to robot-assisted movement," *Proc IEEE RAS EMBS Int Conf Biomed Robot Biomechatron*, vol. 2024, pp. 1670–1675, 2024.

[17] L. L. Van Der Velden, B. Onneweer, C. J. W. Haarman, J. L. Benner, M. E. Roebroeck, G. M. Ribbers, and R. W. Selles, "Development of a single device to quantify motor impairments of the elbow: proof of concept," *Journal of NeuroEngineering and Rehabilitation*, vol. 19, no. 1, p. 77, 7 2022. [Online]. Available: https://doi.org/10.1186/s12984-022-01050-2

[18] H. G. Kortier, V. I. Sluiter, D. Roetenberg, and P. H. Veltink, "Assessment of hand kinematics using inertial and magnetic sensors," *J Neuroeng Rehabil*, vol. 11, p. 70, 2014.

[19] Y. Ye, L. Ma, T. Yan, H. Liu, X. Wei, and R. Song, "Kinetic measurements of hand motor impairments after mild to moderate stroke using grip control tasks," *J Neuroeng Rehabil*, vol. 11, p. 84, 2014.

[20] S. Gibbons, "Design Thinking 101," 4 2024. [Online]. Available: https://www.nngroup.com/articles/design-thinking/

[21] G. Prange, L. Smulders, J. van Wijngaarden, G. Lijbers, S. Nijenhuis, P. Veltink, J. Buurke, and A. Stienen, "User requirements for assistance of the supporting hand in bimanual daily activities via a robotic glove for severely affected stroke patients," *IEEE Transactions on Haptics*, pp. 357–361, 2015.

[22] M. Vergara, J. Sancho-Bru, V. Gracia-Ibáñez, and A. Pérez-González, "An introductory study of common grasps used by adults during performance of activities of daily living," *Journal of Hand Therapy*, vol. 27, no. 3, pp. 225–234, 2014. [Online]. Available: https://www.sciencedirect.com/science/article/pii/S0894113014000520

[23] *FX29 Compact Compression Load Cell — Datasheet (Rev. A8)*, TE Connectivity Sensors, 2025.

[24] M. Arvandi, B. Strasser, C. Meisinger, K. Volaklis, R. M. Gothe, U. Siebert, K.-H. Ladwig, E. Grill, A. Horsch, M. Laxy, A. Peters, and B. Thorand, "Gender differences in the association between grip strength and mortality in older adults: results from the KORA-age study," *BMC Geriatrics*, vol. 16, no. 1, 11 2016. [Online]. Available: https://doi.org/10.1186/s12877-016-0381-4

[25] N. Incel, E. Ceceli, P. Durukan, H. Erdem, and Z. Yorgancioglu, "Grip strength: Effect of hand dominance," *Singapore medical journal*, vol. 43, pp. 234–7, 06 2002.

[26] V. Mathiowetz, K. Weber, G. Volland, and N. Kashman, "Reliability and validity of grip and pinch strength evaluations," *The Journal Of Hand Surgery*, vol. 9, no. 2, pp. 222–226, 3 1984. [Online]. Available: https://pubmed.ncbi.nlm.nih.gov/6715829/

[27] C. A. Celis-Morales, F. Petermann, L. Hui, D. M. Lyall, S. Iliodromiti, J. McLaren, J. Anderson, P. Welsh, D. F. Mackay, J. P. Pell, N. Sattar, J. M. Gill, and S. R. Gray, "Associations between diabetes and both cardiovascular disease and all-cause mortality are modified by grip strength: Evidence from uk biobank, a prospective population-based

cohort study," *Diabetes Care*, vol. 40, no. 12, pp. 1710–1718, 10 2017. [Online]. Available: https://doi.org/10.2337/dc17-0921

[28] M. Kim and S. Shinkai, "Prevalence of muscle weakness based on different diagnostic criteria in community-dwelling older adults: A comparison of grip strength dynamometers," *Geriatrics and gerontology international/Geriatrics gerontology international*, vol. 17, no. 11, pp. 2089–2095, 5 2017. [Online]. Available: https://doi.org/10.1111/ggi.13027

[29] T. Watanabe, K. Owashi, Y. Kanauchi, N. Mura, M. Takahara, and T. Ogino, "The Short-Term reliability of grip strength measurement and the effects of posture and grip span," *The Journal Of Hand Surgery*, vol. 30, no. 3, pp. 603–609, 5 2005. [Online]. Available: https://pubmed.ncbi.nlm.nih.gov/15925174/

[30] K. Konharn, T. Chaichan, A. Leungbootnak, J. Karawa, and K. Udomtaku, "Interval rest period and different testing positions on hand-grip strength measurement among young adults," 2018. [Online]. Available: https://he01.tci-thaijo.org/index.php/ams/article/view/163939

[31] M. Taga, N. Ushiyama, Y. Kurobe, and K. Momose, "How much rest period is needed between measurements in the repeated measures of maximum isometric knee extension strength?" *Physiotherapy*, vol. 101, p. e1466, 5 2015. [Online]. Available: https://doi.org/10.1016/j.physio.2015.03.1434

[32] E. Innes, "Handgrip strength testing: A review of the literature," *Australian Occupational Therapy Journal*, vol. 46, no. 3, pp. 120–140, 9 1999. [Online]. Available: https://doi.org/10.1046/j.1440-1630.1999.00182.x

[33] N. J. Seo and T. J. Armstrong, "Fingertip force production during static power grip," *Ergonomics*, vol. 54, no. 11, pp. 1039–1050, 2011.

[34] R. W. Bohannon and A. W. Andrews, "Distribution of grip force in three different functional prehension patterns," *Journal of Hand Therapy*, vol. 19, no. 4, pp. 372–376, 2006.

[35] K. Li, P. Zhang, and Y. Zheng, "An analysis of fingertip force distribution during cylindrical grasping," *Journal of Biomechanics*, vol. 38, no. 8, pp. 1600–1605, 2005.

[36] H. Kinoshita, "Fingertip force-sharing patterns during precision grip in humans," *Journal of Biomechanics*, vol. 20, no. 3, pp. 231–242, 1987.

[37] V. M. Zatsiorsky and M. L. Latash, "Multi-finger prehension: biomechanics, neural control and clinical implications," *Journal of Neurophysiology*, vol. 104, no. 3, pp. 1155–1167, 2010.

[38] M. S. Sanders and E. J. McCormick, *Human factors in engineering and design*. MCGRAW HILL BOOK CO, 1 1957. [Online]. Available: http://ci.nii.ac.jp/ncid/BA20646912

[39] A. Yurkewich, I. J. Kozak, D. Hebert, R. H. Wang, and A. Mihailidis, "Hand Extension Robot Orthosis (HERO) Grip Glove: enabling independence amongst persons with severe hand impairments after stroke," *Journal of NeuroEngineering and Rehabilitation*, vol. 17, no. 1, 2 2020.

[40] V. Nazari, M. Pouladian, Y.-P. Zheng, and M. Alam, "A Compact and Lightweight Rehabilitative Exoskeleton to Restore Grasping Functions for People with Hand Paralysis," *Sensors*, vol. 21, no. 20, p. 6900, 10 2021. [Online]. Available: https://doi.org/10.3390/s21206900

[41] T. Murai, S. Uchiyama, K. Nakamura, Y. Ido, Y. Hata, and H. Kato, "Functional range of motion in the metacarpophalangeal joints of the hand measured by single axis electric goniometers," *Journal of Orthopaedic Science*, vol. 23, no. 3, pp. 504–510, 2 2018. [Online]. Available: https://doi.org/10.1016/j.jos.2018.01.013

[42] R. Alhamad, N. Seth, and H. A. Abdullah, "Initial testing of robotic exoskeleton hand device for stroke rehabilitation," *Sensors*, vol. 23, no. 14, p. 6339, 7 2023. [Online]. Available: https://doi.org/10.3390/s23146339

[43] M. Caeiro-Rodríguez, I. Otero-González, F. A. Mikic-Fonte, and M. Llamas-Nistal, "A Systematic Review of Commercial smart gloves: Current status and applications," *Sensors*, vol. 21, no. 8, p. 2667, 4 2021. [Online]. Available: https://doi.org/10.3390/s21082667

[44] P. Kanade-Mehta, M. Bengtson, T. Stoeckmann, J. McGuire, C. Ghez, and R. A. Scheidt, "Spatial mapping of posture-dependent resistance to passive displacement of the hypertonic arm post-stroke," *Journal of NeuroEngineering and Rehabilitation*, vol. 20, no. 1, 12 2023. [Online]. Available: https://doi.org/10.1186/s12984-023-01285-7

[45] I. M. Bullock, J. Z. Zheng, S. De La Rosa, C. Guertler, and A. M. Dollar, "Grasp frequency and usage in daily household and machine shop tasks," *IEEE Transactions on Haptics*, vol. 6, no. 3, pp. 296–308, 2013.

APPENDIX

APPENDIX A

INITIAL REQUIREMENTS

TABLE IV: Overview of initial User, Researcher, and Therapist Requirements

No.	Requirement	Preference / Specification	Actor
1	Device should be suitable for anthropometry of 90% of the adult population	5th–95th percentile [38]	User
2	Doffing and donning of the device should be possible within 5 minutes	$\leq$ 5 min [39]	User
3	Device should not constrain finger movement and must allow predefined grasps	–	User
4	Device must actuate hand extension across functional ranges of motion	MCP: 19°–71°, PIP: 23°–87°, DIP: 10°–64° [40]	User
5	Device should be made of skin-friendly materials	–	User
6	Device must be safe, avoiding joint misalignment and exceeding safe limits of motion	MCP: Hyperextension 45°, Flexion 90° [41]	User
7	Device must be able to generate sufficient force to extend impaired fingers	$\geq$ 26 N [42]	User
8	Device should be modular for easy repair and adjustment	–	Researcher
9	Device must be able to measure grip force	Distribution of force per finger	Researcher
10	Device must be mountable on a 20$\times$40 mm aluminium profile	–	Researcher
11	Device should have a high temporal resolution (sample rate)	$\geq$ 75 Hz [43]	Researcher
12	Device should supply variable actuation forces for passive assessment	0–26 N	Researcher
13	Device must output measurable data such as angle (°) or force (N)	–	Therapist
14	Device must allow both passive and active assessment	–	Therapist
15	Device should provide patient feedback (visual, auditory, or haptic)	–	Therapist
16	During passive assessment, the device must support variable movement speeds	6°/s–90°/s [44]	Therapist

APPENDIX B

MORPHOLOGICAL CHART

This appendix presents the morphological chart developed during the *Ideate* phase. It summarizes the technical alternatives explored for each major subfunction of the force measurement system.

TABLE V: Morphological chart of subfunctions and possible technical solutions.

Subfunction	**1**	**2**	**3**	**4**	**5**	**6**	**7**	**8**	**9**	**10**	**11**
Measurement of Force	Dynamometer	Spring deflection	Force sensor	Strain gauge (load cell)	Pressure cell	DC motor torque	Torque–current relation	Torque–speed relation	Tactile sensor	–	–
Actuated Hand Extension	Linear motor	DC motor	Springs	Cable driven	Linkage driven	Rotating platform	Expanding element	Pneumatic	EMG	Spindle	–
Modular Base Geometry	Aluminium profile	Threaded connection	Click system	Velcro	Form fitted	Clamped	Friction based	Nuts and bolts	Tape	–	–
Hand Aperture Measurement	IMU	Accelerometer	Gyroscope	Bend sensor	Motion capture	Rotary encoder	IR distance sensor	Ultrasonic sensor	Slider	Linear encoder	Stepper motor
Grasp Object Design	Sphere	Cube	Cylinder	Cone	Flat plate	–	–	–	–	–	–
Adaptability to Hand Sizes	Modular components	Velcro attachment	Item-based adjustment	Interchangeable sizes	Adjustable parts	Slider mechanism	Rotational mechanism	–	–	–	–
Finger Distribution Measurement (Optional)	Pressure sensors (surface)	Separate sensor per finger	–	–	–	–	–	–	–	–	–

APPENDIX C

CONCEPT DEVELOPMENT AND EVALUATION

This appendix presents an overview of the five preliminary design concepts developed during the *Ideate* phase. Each concept combines different sensing and actuation principles derived from the morphological chart (Appendix B). For every concept, the main principle and representative CAD visualizations are shown.

Concept 1 — Rotating Cylinder Mechanism

A cylindrical mechanism that opens the hand through rotation using a DC motor. The concept enables a natural extension movement while measuring fingertip pressure using integrated sensors.

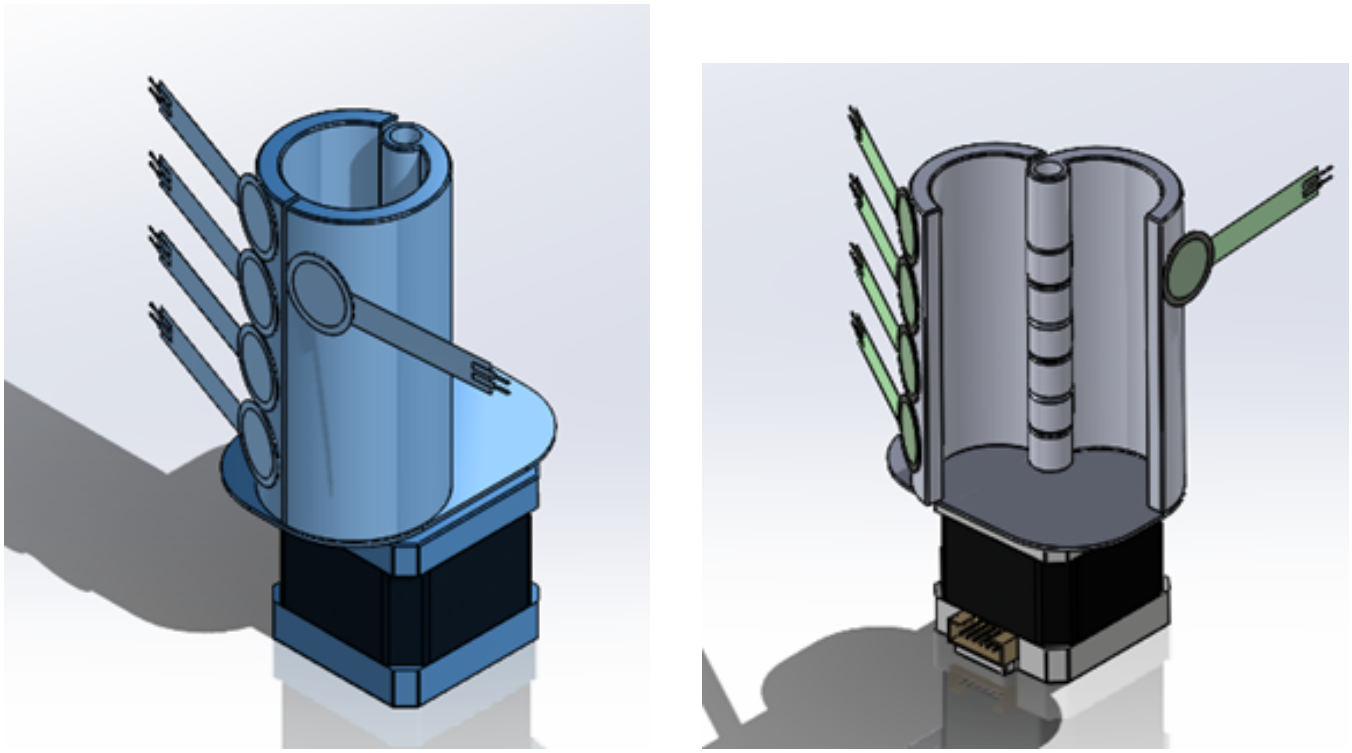

(a) Closed configuration. (b) Hand extension configuration.

Fig. 13: Concept 1 – Rotating Cylinder Mechanism.

Concept 2 — Dynamometer-Inspired Device

Based on a conventional hand dynamometer, this concept integrates a linear actuator and load cell to measure total and distributed grip forces.

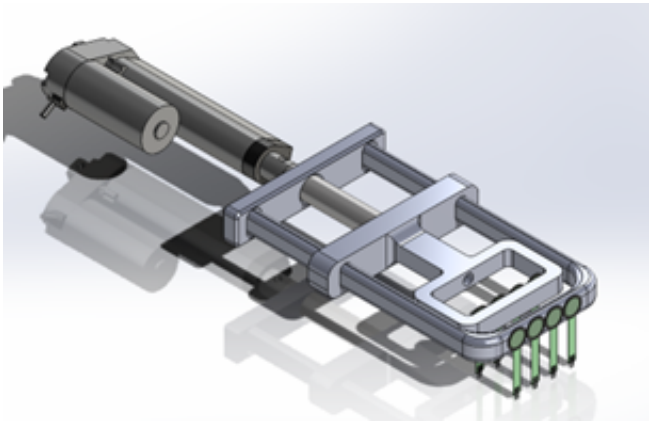

(a) Closed configuration.

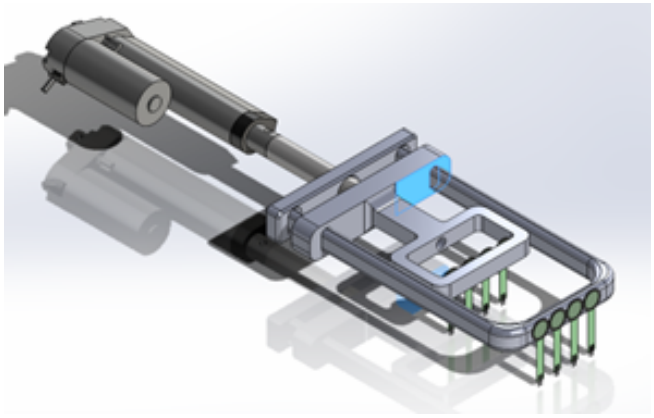

(b) Open configuration during hand extension.

Fig. 14: Concept 2 – Dynamometer-Inspired Device.

Concept 3 — Cable-Driven Mechanism

A gear-and-cable driven system enabling both flexion and extension. Each finger is connected to a dedicated load cell, allowing individual force measurement.

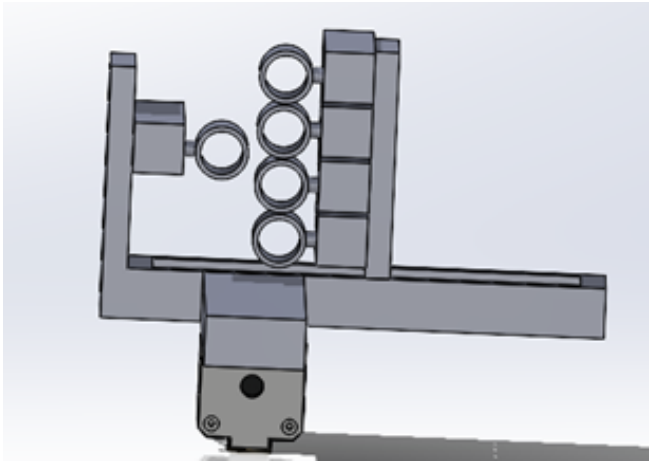

(a) Resting configuration.

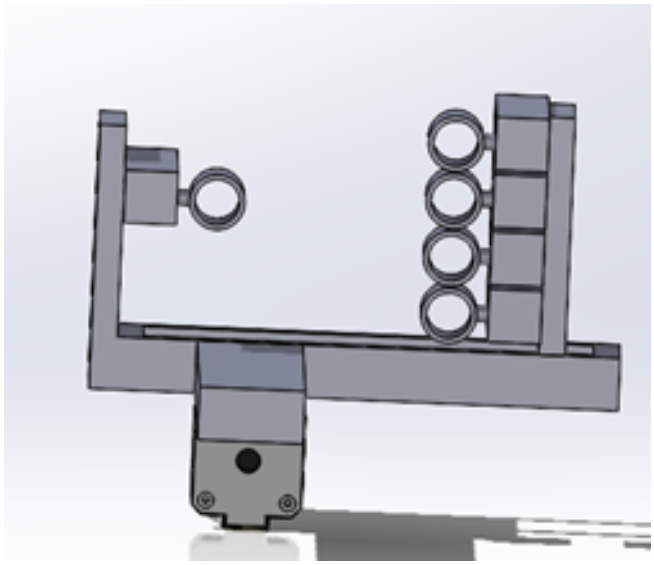

(b) Actuated configuration.

Fig. 15: Concept 3 – Cable-Driven Mechanism.

Concept 4 — Pressure-Slab Mechanism

A passive design replacing finger rings with a pressure-sensitive slab to improve comfort and adaptability across hand sizes.

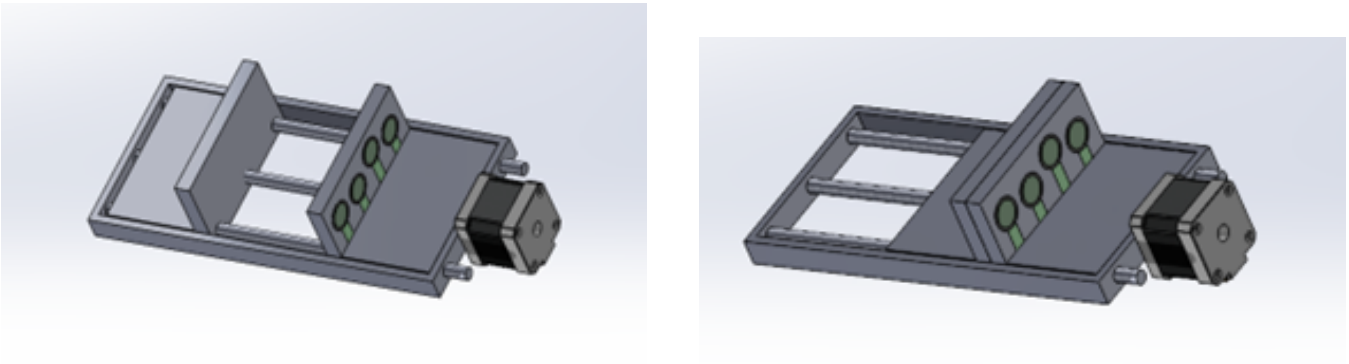

(a) Closed configuration. (b) Open configuration.

Fig. 16: Concept 4 – Pressure-Slab Mechanism.

Concept 5 — Exoskeleton Mechanism

A lightweight exoskeleton actuated by cable tension to produce finger flexion. Forces are measured at the fingertip sensors, and cable tension represents total output force.

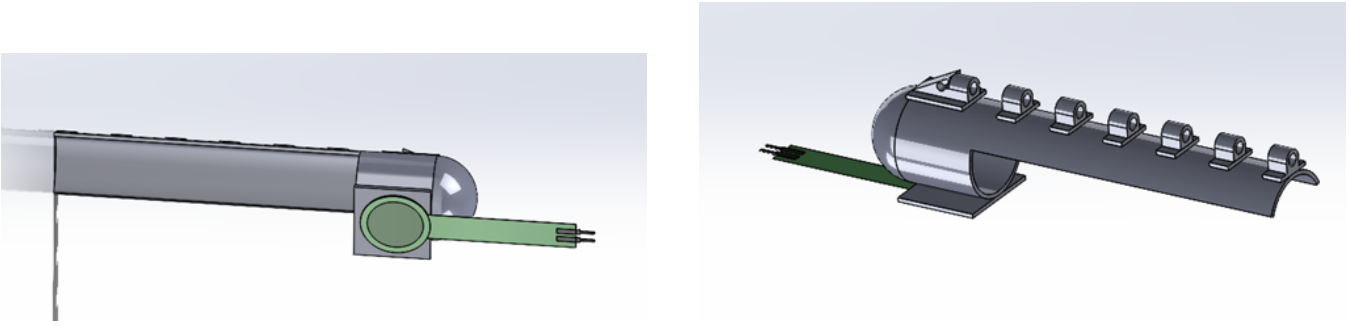

(a) Side view of exoskeleton layout. (b) Front view showing cable-based actuation.

Fig. 17: Concept 5 – Exoskeleton Mechanism.

A comparative assessment of these five concepts, including scoring and selection rationale, is provided in the following section of this appendix.

Each concept was scored from 1 (poor) to 5 (excellent) for every criterion. The weighted scores were then summed to yield the total performance index of each concept.

TABLE VI: Condensed weighted scoring comparison of the five design concepts with visual reference and descriptive names.

Criterion (Weight)	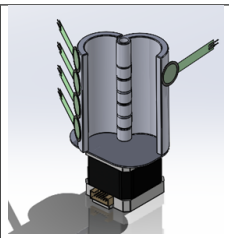 **Rotating Cylinder**	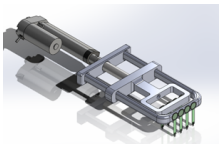 **Dynamometer-Inspired**	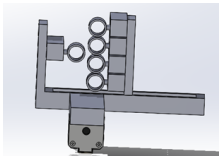 **Cable-Driven**	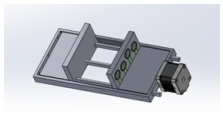 **Pressure-Slab**	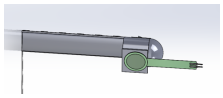 **Exoskeleton**
Safety (10)	2	4	4	**5**	4
Measurement Accuracy (8)	3	**5**	4	3	2
Actuation Performance (7)	2	3	**5**	5	4
Anthropometric Coverage (6)	2	4	3	**5**	2
Ergonomic Comfort (5)	**5**	4	2	4	3
Ease of Use (4)	**5**	4	3	5	2
Modularity (3)	2	2	**5**	4	5
Weight (2)	**5**	2	2	3	4
Cost (1)	**5**	1	3	3	2
Total Weighted Score	136	172	169	**200**	144

The results show that **Concept 4 (Pressure-Slab Mechanism)** achieved the highest overall score, driven by its balance of safety, modularity, and ergonomic adaptability. While it met the functional objectives of distributed force measurement, subsequent prototyping revealed issues of excessive mass and lateral shear forces, which guided the second design iteration described in Section II.

==========

APPENDIX D

GRASP TYPE DIAGRAMS

This appendix provides the grasp-duration distributions of the top 10 grasps identified in daily bimanual activities. The histograms and fitted kernel density curves illustrate the relative frequency and mean duration of each grasp type as reported by Bullock et al. [45].

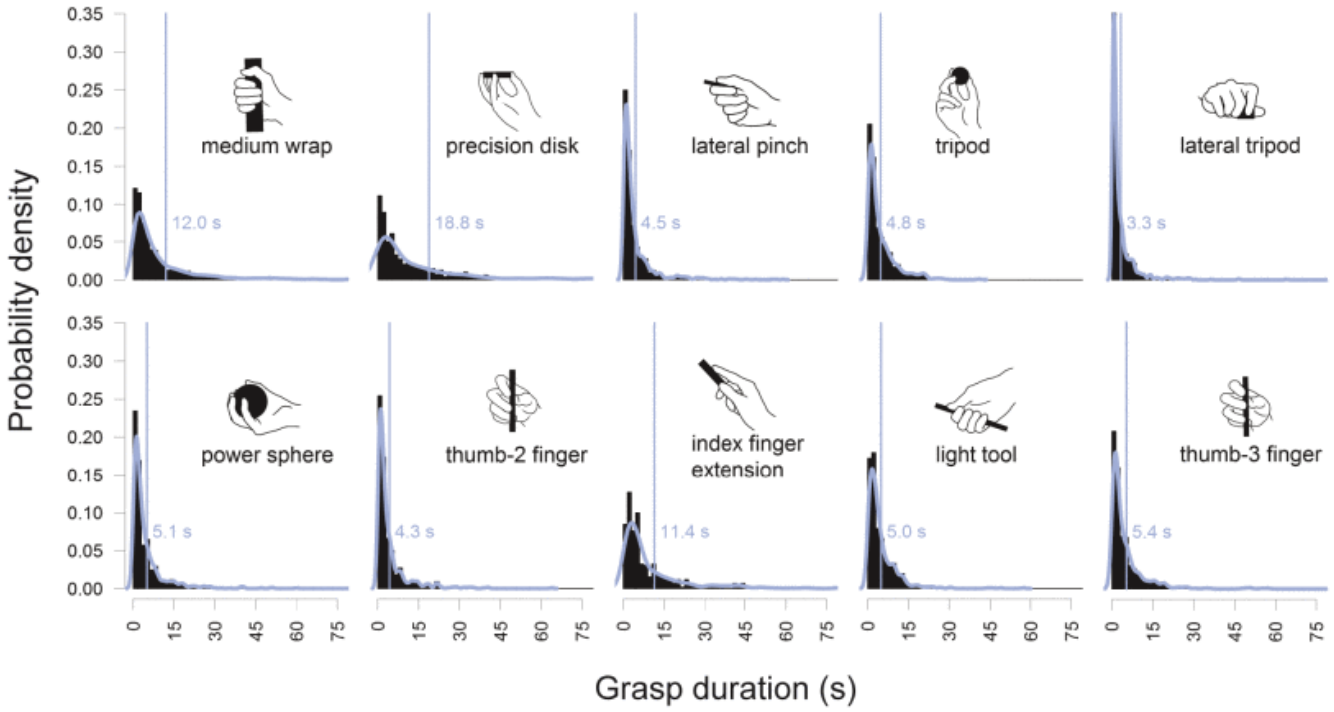

Fig. 18: Grasp duration histograms for the top 10 grasps. Kernel density curves are fitted for each histogram, and the labeled line corresponds to the mean duration for each grasp. [45]

APPENDIX E

DIMENSIONED DRAWINGS OF THE FINAL PROTOTYPE

This appendix presents the external dimensions of the final device configuration, including the lateral thumb-module attachment used for the medium-wrap grasp. All drawings were exported from the final CAD model and illustrate the principal overall dimensions referenced in Section III.

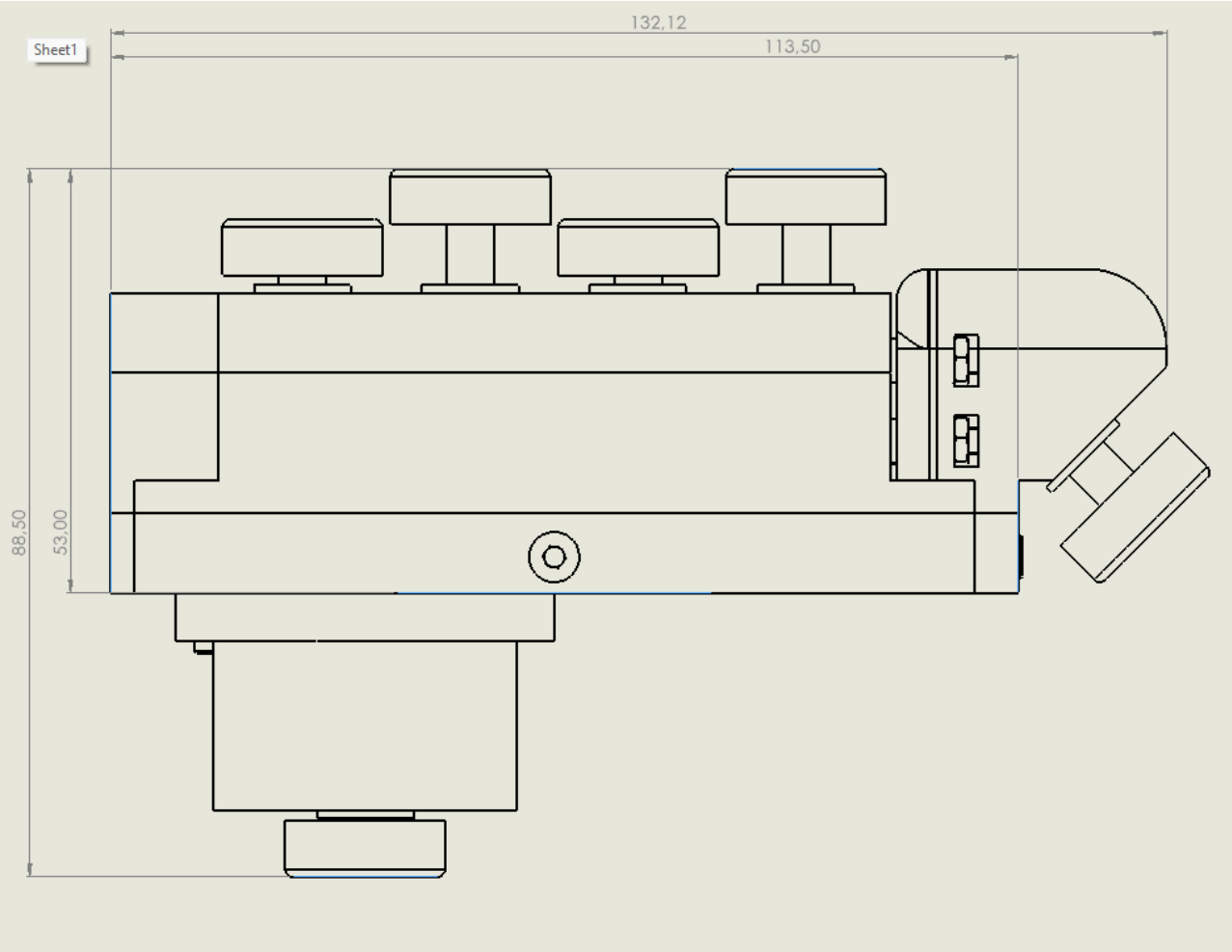

Fig. 19: Side view of the final prototype with the lateral thumb module attached. The total length is 132.1 mm and the maximum height is 88.5 mm (53 mm excluding pistons).

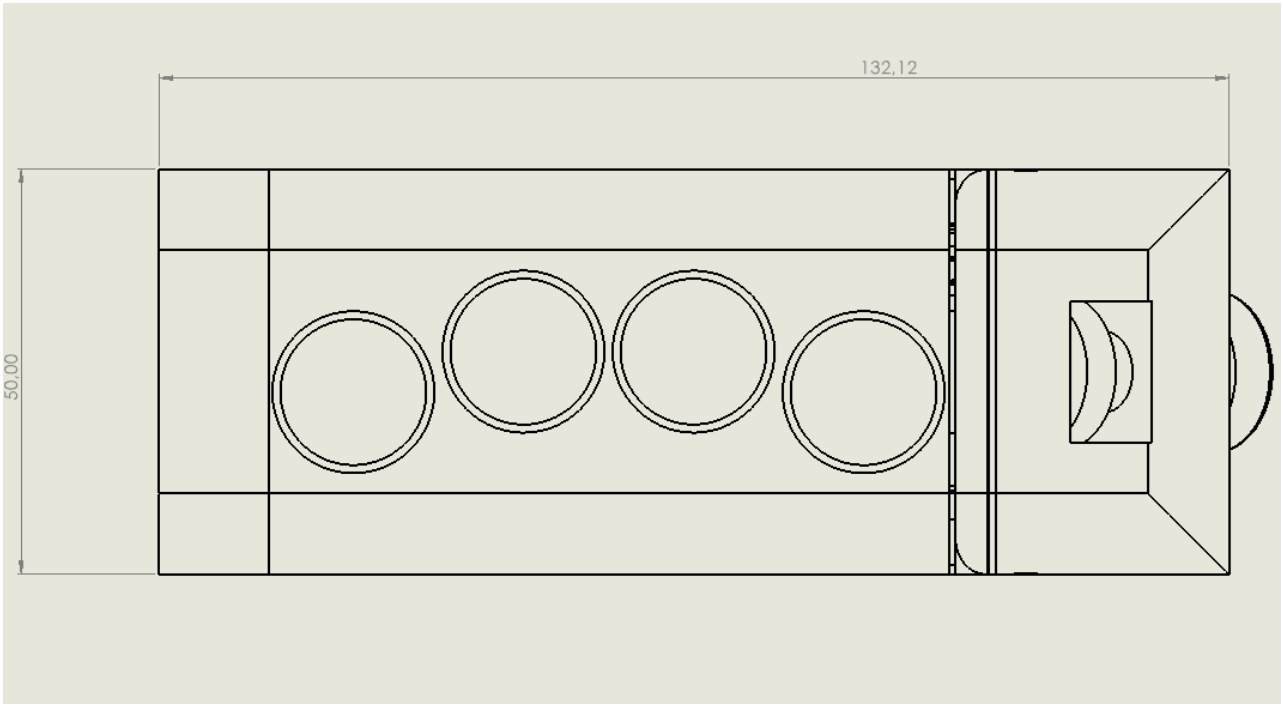

Fig. 20: Top view of the final prototype showing the four finger piston housings and the lateral thumb attachment. The overall footprint measures 132.1 mm in length and 50 mm in width.

APPENDIX F

FREE-BODY DIAGRAMS OF GRASP CONFIGURATIONS

This appendix provides the full free-body diagrams of the device under both grasp conditions, illustrating the interaction between the thumb and fingers, as well as the internal forces transmitted through each piston–spring–sensor assembly.

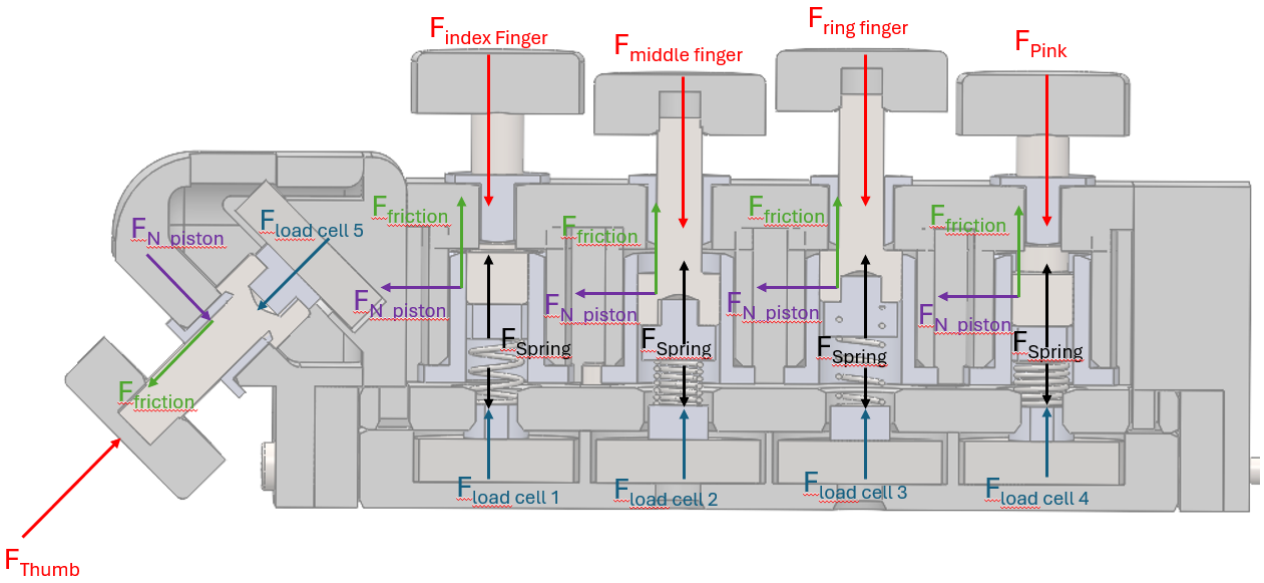

Fig. 21: Free-body diagram of the medium-wrap grasp configuration showing the load transfer from all fingers and the thumb module.

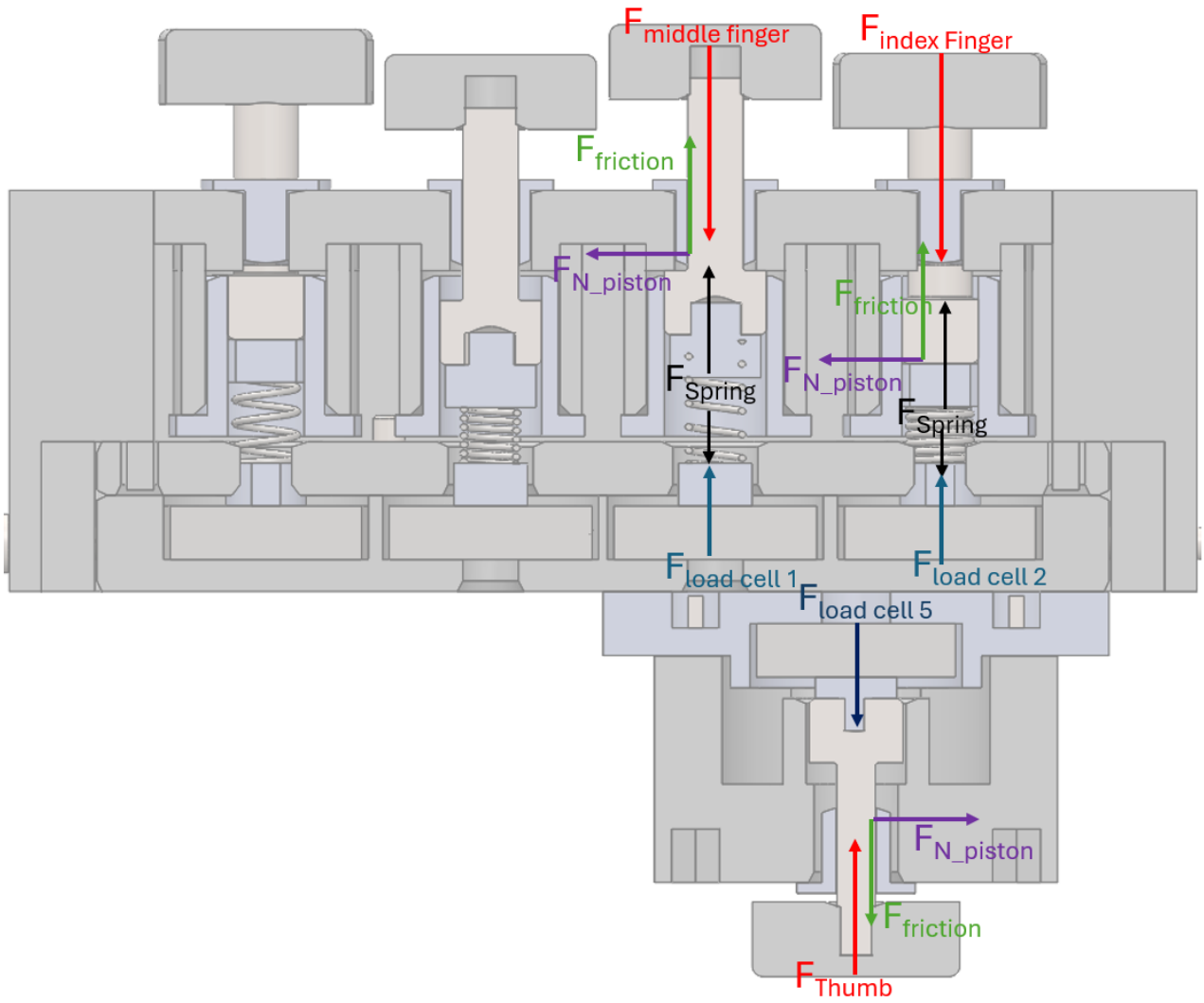

Fig. 22: Free-body diagram of the precision-disk grasp configuration illustrating the opposed load paths between the thumb and the index–middle finger modules.

APPENDIX G

ELECTRICAL WIRING AND COMMUNICATION LAYOUT

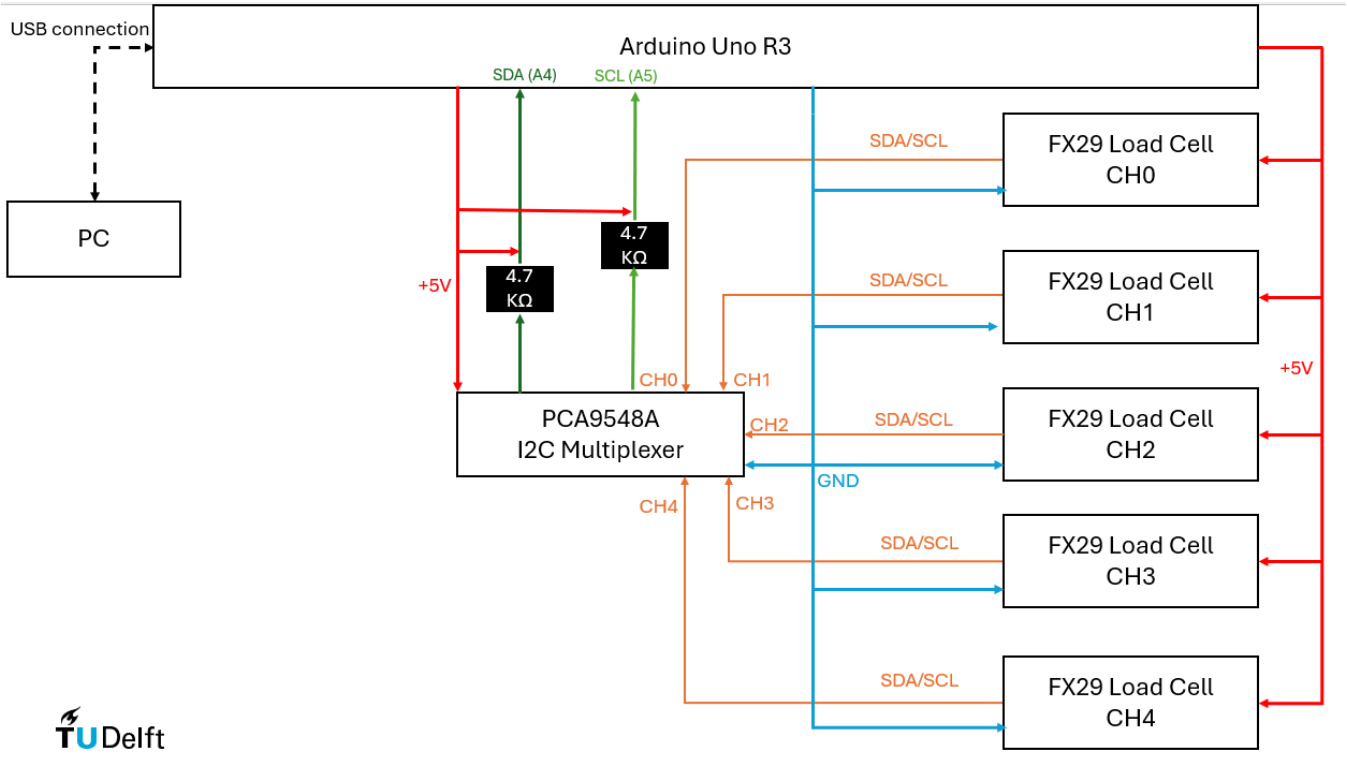

Fig. 23: Clean wiring schematic. USB (black dashed) connects PC to Arduino. +5 V (red) and GND (blue) originate from the Arduino, feed the Multiplexer, and the five FX29 load cells. SDA/SCL (Orange) use 4.7 kΩ pull-ups and are routed via the multiplexer to CH0–CH4.

APPENDIX H
REAL CALIBRATION TEST SETUP

This appendix provides the full calibration methodology, validation results, and low-load improvement steps underlying the summary presented in Section IV.

A. Calibration Procedure

Each FX29 load cell was calibrated using a rope-and-weight loading mechanism in which known masses were applied through a piston attached to the sensor. The calibration aimed to establish a sensor-specific mapping from the 14-bit digital output to force (N). Two physical configurations were used during calibration:

- **Leveled configuration**: the pulley and sensor housing were aligned horizontally to establish a baseline calibration 24a.
- **15° inclined configuration**: replicating the device's operational orientation and used to assess the sensitivity to partial off-axis loading 24b.

In both configurations, a zero-load reference was recorded including the piston, rope, and container. Five mass steps (0 g, 500 g, 990 g, 1490 g, 2043 g) were sequentially applied and repeated three times to verify stability. For each step, the raw sensor counts were logged and used to compute the calibration slope (counts/N) and corresponding interpolation function.

(a) Leveled configuration.

(b) 15° inclined configuration.

Fig. 24: Calibration rigs used during sensor characterization: (a) leveled and (b) inclined configuration.

B. Live Data Validation

To verify the stability and accuracy of the derived calibration curves, each sensor was evaluated under continuous loading at 100 Hz. The same load steps as during calibration were applied, with an additional 2530 g load to assess interpolation accuracy beyond the calibrated range.

For each step, the measured force was compared to the known load, and the mean and maximum errors were computed relative to the full-scale (FS) rating of the FX29 sensor. An example validation curve for Sensor 2 is shown in Figure 25.

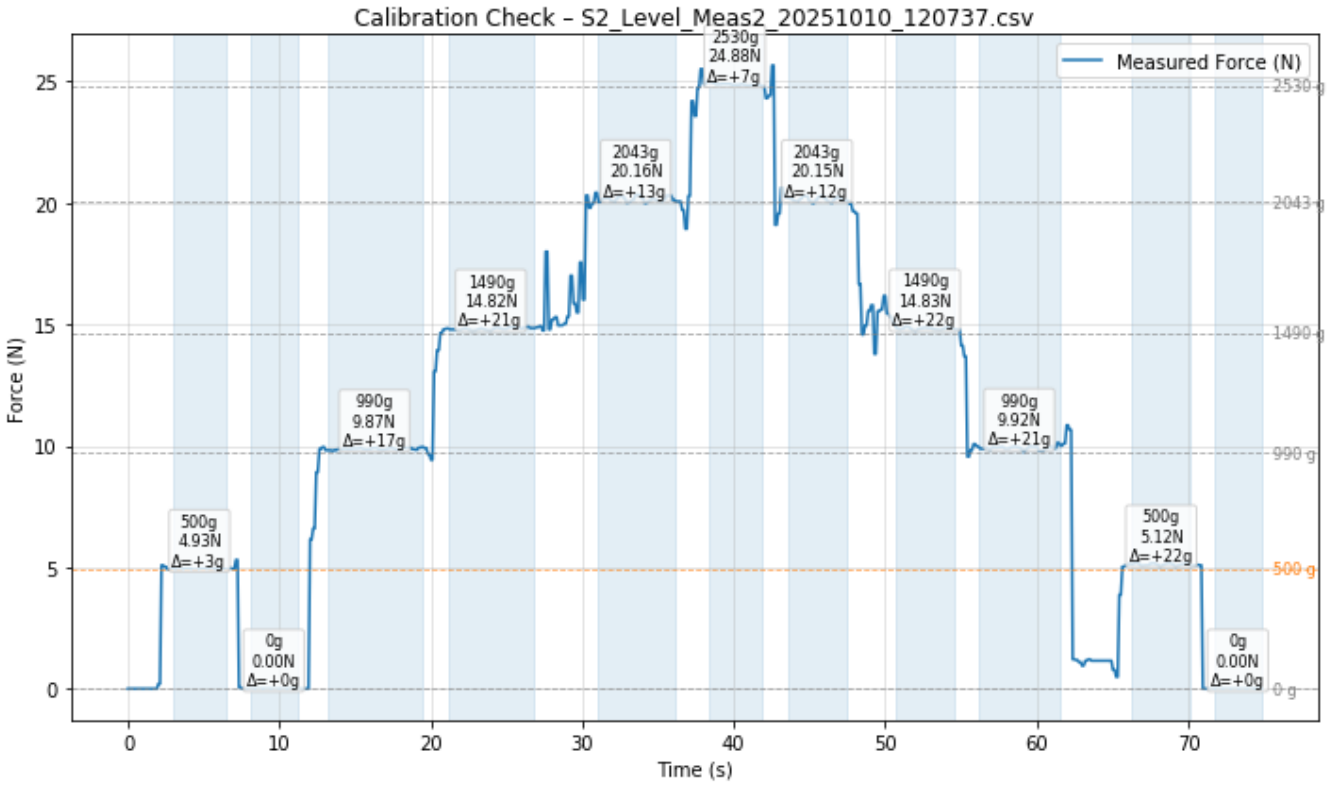

Fig. 25: Example validation trial for Sensor 2 showing measured vs. applied force.

Error metrics across all sensors are summarized in Figure 26. Both the average and peak errors remained within the 0–1 %FS accuracy range specified by the manufacturer, confirming robust performance under both axial and moderately off-axis loading conditions.

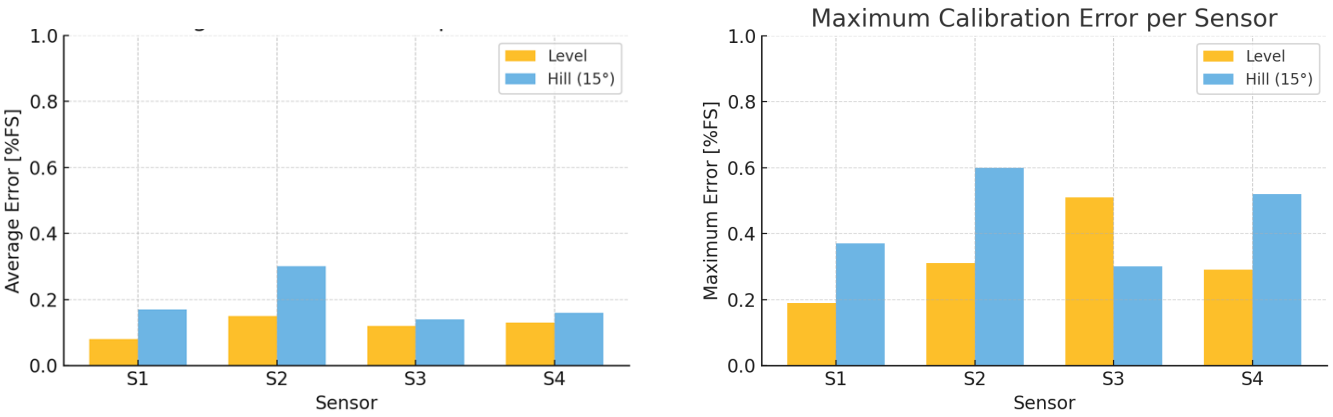

(a) Average calibration error per sensor.

(b) Maximum calibration error per sensor.

Fig. 26: Summary of calibration errors across three repeated trials.

C. Low-Load Range Improvement

Initial validation revealed increased measurement variability in the 0–1 kg range. This was attributed to static friction between the piston and bearing interface at low spring compression and to the relatively sparse distribution of calibration points in this region.

To address these issues, several mechanical and procedural refinements were introduced:

- **Lubrication** of the piston and sliding interfaces to reduce friction and stick–slip.
- **Redesigned spring holders** manufactured from laser-cut PMMA to improve axial alignment and structural stiffness.
- **An expanded low-weight calibration scheme** including: 200 g, 250 g, 450 g, 500 g, 700 g, 750 g, and 990 g.

A complete re-validation was performed using the same 100 Hz live measurement procedure. The refined calibration significantly improved accuracy in the low-load range. Figure 27 shows that the mean calibration error decreased from 0.21 %FS to 0.10 %FS (approximately 52 % reduction), with all sensors comfortably within the 1 %FS specification.

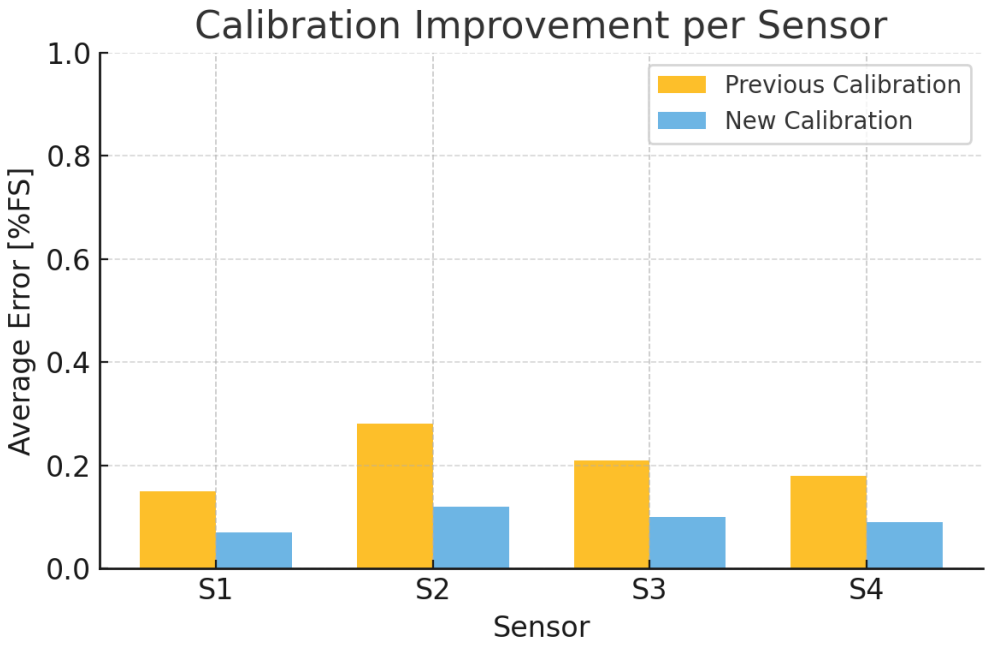

Fig. 27: Average calibration error before and after refinement, averaged across sensors.

This improved calibration set was used as the reference for all subsequent user testing described in the main body of this thesis.

APPENDIX I

INDIVIDUAL SD'S OF DYNAMOMETER VS DEVICE PER SUBJECT PER GRASP

This appendix presents the per-subject standard deviation (SD) values for each grasp type, illustrating the trial-to-trial repeatability of both the device and the reference dynamometer. For every participant, the SD of all recorded trials is shown for the device (blue) and for the dynamometer (gray). These plots provide a detailed overview of the individual variability across subjects and grasp types, complementing the group-level repeatability results reported in the main text.

Summary and Interpretation

Figures 28, 29, 30 and 31 show that the SD values vary noticeably between subjects, which is expected in repeated maximal-effort grip tasks. The key question is whether the device introduces additional variability compared to the dynamometer. Based on the results, this is not the case.

For **Medium Wrap**, the dynamometer SDs range roughly from 8–35 N, while the device SDs fall in a very similar range of 11–30 N. Some subjects (e.g. S3, S9 and S11) show a lower SD on the dynamometer and a higher SD on the device, while the opposite is seen for others (e.g. S4 and S6). There is no consistent pattern where one instrument is always more variable.

For **Precision Disk**, the dynamometer shows consistently low SD values (around 1–6 N), whereas the device SD is slightly higher (5–13 N). This difference is expected, since the dynamometer measures a single-point pinch force, while the device measures a three-finger precision grip. Even so, the SDs for both instruments remain small.

For **Power Grasp**, the comparison is roughly balanced. Some subjects show a higher SD on the dynamometer (e.g. S3, S6, S10 and S11), while others have a higher SD on the device (e.g. S1, S4 and S7). Again, no consistent bias is present.

When averaging the SD values across all subjects (Figure 28), the device and the dynamometer end up at almost the same level for all grasp types:

- Medium Wrap: 19.1 N (dyn) vs. 20.8 N (device)
- Precision Disk: 3.6 N (dyn) vs. 9.2 N (device)
- Power Grasp: 17.3 N (dyn) vs. 13.8 N (device)

These averages confirm that the device captures repeatability on the same order of magnitude as the dynamometer. The differences observed between subjects are dominated by normal human trial-to-trial variation rather than measurement noise. Overall, the device achieves a repeatability level that is comparable to the established reference instrument.

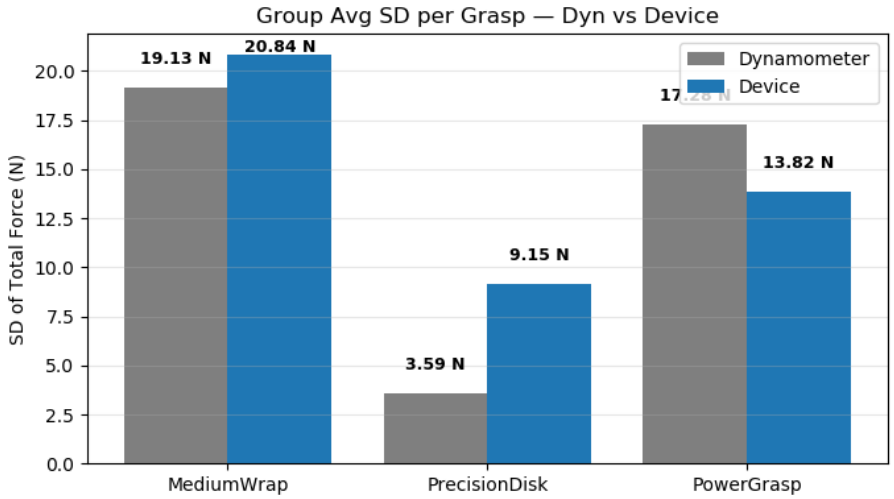

Fig. 28: Average standard deviation per grasp for all subjects

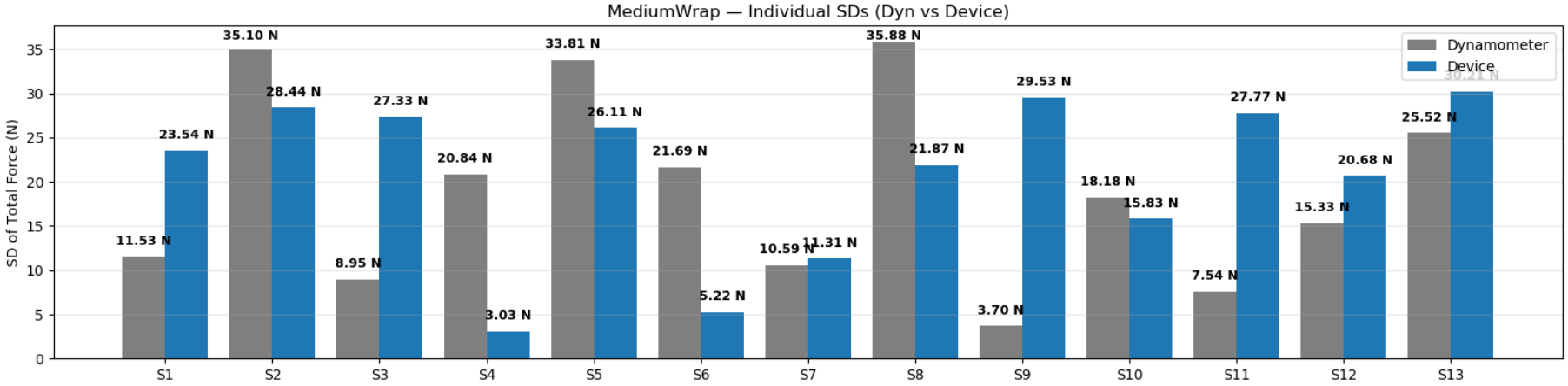

Fig. 29: Medium Wrap grasp: individual SD per subject for the device (blue) and dynamometer (gray).

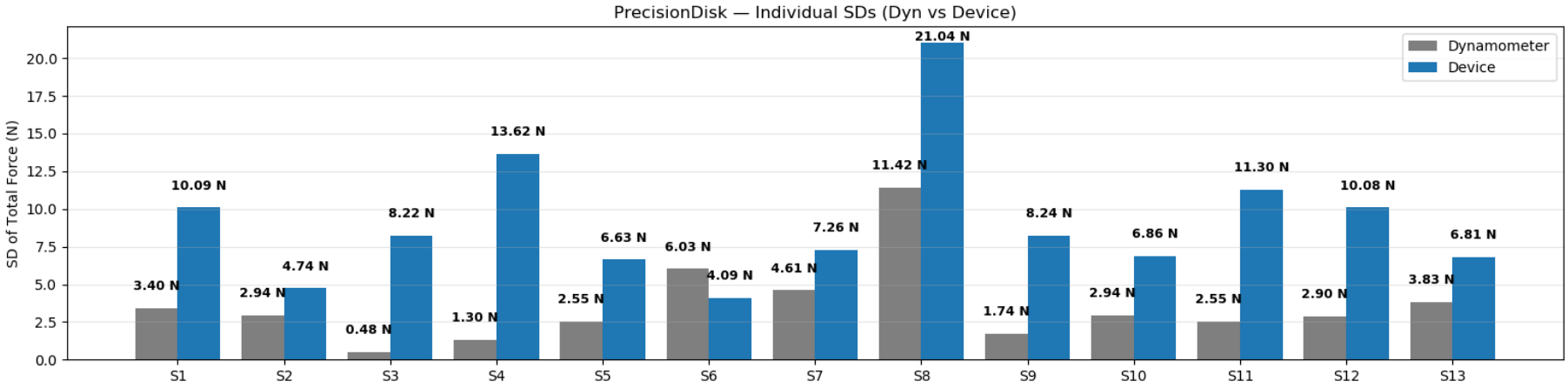

Fig. 30: Precision Disk grasp: individual SD per subject for the device (blue) and dynamometer (gray).

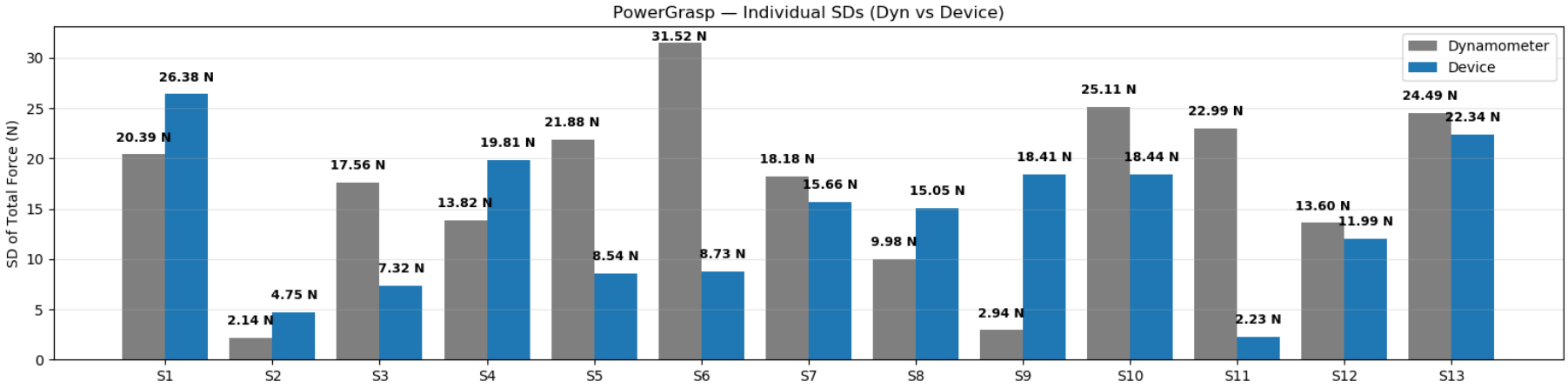

Fig. 31: Power Grasp: individual SD per subject for the device (blue) and dynamometer (gray).

APPENDIX J

PARTICIPANT INFORMATION AND INFORMED CONSENT

This appendix contains the full participant-information document provided to all volunteers prior to the study, as well as the informed consent form that each participant signed in accordance with the Human Research Ethics Committee (HREC) guidelines.

Participant information – Hand assessment device usability study

You are invited to participate in the study '*Evaluation of a Hand Assessment Device for Measuring Finger Forces.*' This study is conducted by Jasper van Aernsbergen, MSc student at TU Delft, Faculty of Mechanical Engineering.

Study objective

The objective of this study is to validate the functionality, anthropometric fit, and ergonomics of a newly developed hand assessment device. The goal is to determine whether the device performs as intended and provides a comfortable fit for users. All collected data will be used solely for device evaluation and development, and will not be applied in clinical trials or patient-related studies.

What is expected of you?

During a session of approximately **30-45 minutes**, you will be asked to perform a series of predefined grasp tasks using **your dominant hand only**.

The tasks include:

- **Medium wrap grip**: This consists of placing the four fingers (index, middle, ring, and little finger) on top of the device, with the thumb placed on the side at an angle of 45 degrees. (see Figure 2)
- **Power grip:** Place the four fingers over the device and wrap your thumb around the device (see Figure 4)
- **Precision disk grip**: Place the index and middle finger on top of the device, with the thumb placed underneath to oppose them.(see Figure 6)
- **Grip strength with hand dynamometer**: You will perform maximal voluntary contractions of all three grasps using a hand dynamometer. These measurements will be performed three times and serve as a validated reference (zero measurement) to compare against the outputs of the hand assessment device. (see figure 1, 3 and 5)

Before each set of measurements, you will complete **one familiarization trial** to get used to the task, followed by **three to four recorded trials** per grasp. Each recorded trial will last **3 seconds** at maximum voluntary force (wait for the beep to finish), with a **minimum of 60 seconds rest** between trials to prevent fatigue.

After completing the grasp tasks, you will be asked to fill in a short **questionnaire** about comfort, hand placement, and the overall usability of the device.

What data will be acquired

During the experiments, the device will record finger force data. Grip strength values from the hand dynamometer will also be collected. In addition, we will record your age group (e.g., 18–25, 25–35), sex, hand dominance. Your responses to the usability questionnaire will be included.

What happens to the data

Your data will be pseudonymized and will not be directly linked to your name, which will only appear on the consent form. Only non-identifiable information such as your age group, sex, hand dominance will be recorded. This reduces the possibility of re-identification.

The collected data will be used exclusively for the purpose of this MSc thesis to evaluate the functionality and ergonomics of the hand assessment device. The data will not be published. All data will be securely stored on TU Delft project drives.

What are the risks associated with this study?

Risks are minimal. You may experience mild hand fatigue or slight discomfort during gripping. These will be mitigated by keeping trials short, providing rest between trials, and allowing you to stop at any moment. The device has been designed to avoid sharp edges and pinch points. If you have a hand injury, you are advised not to participate.

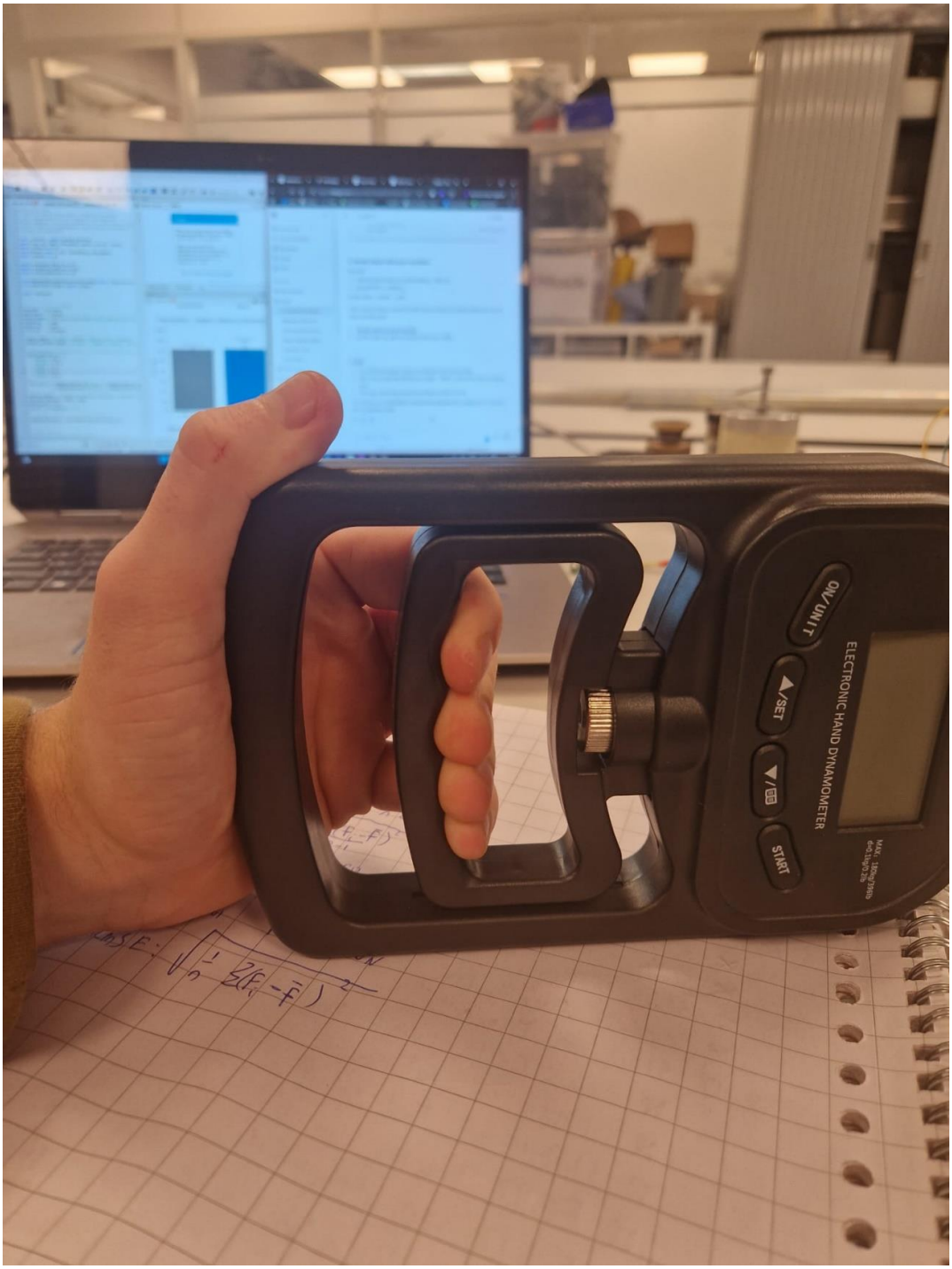

Figure 1: Medium wrap grip - dynamometer

Figure 2: Medium wrap grip - device

Figure 3: Power grip - dynamometer

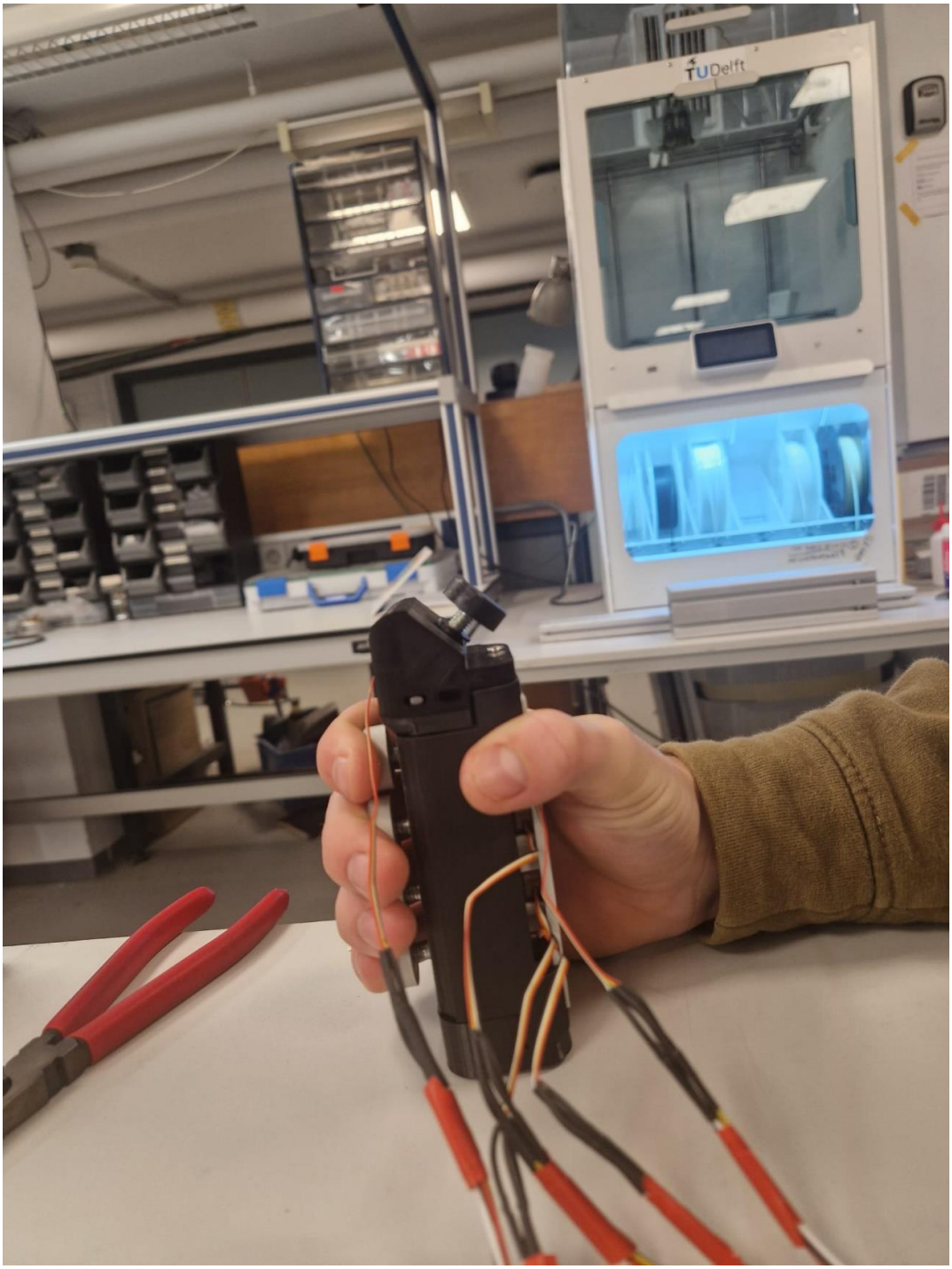

Figure 4: Power grip - device

Figure 5: Precision disk grasp - dynamometer

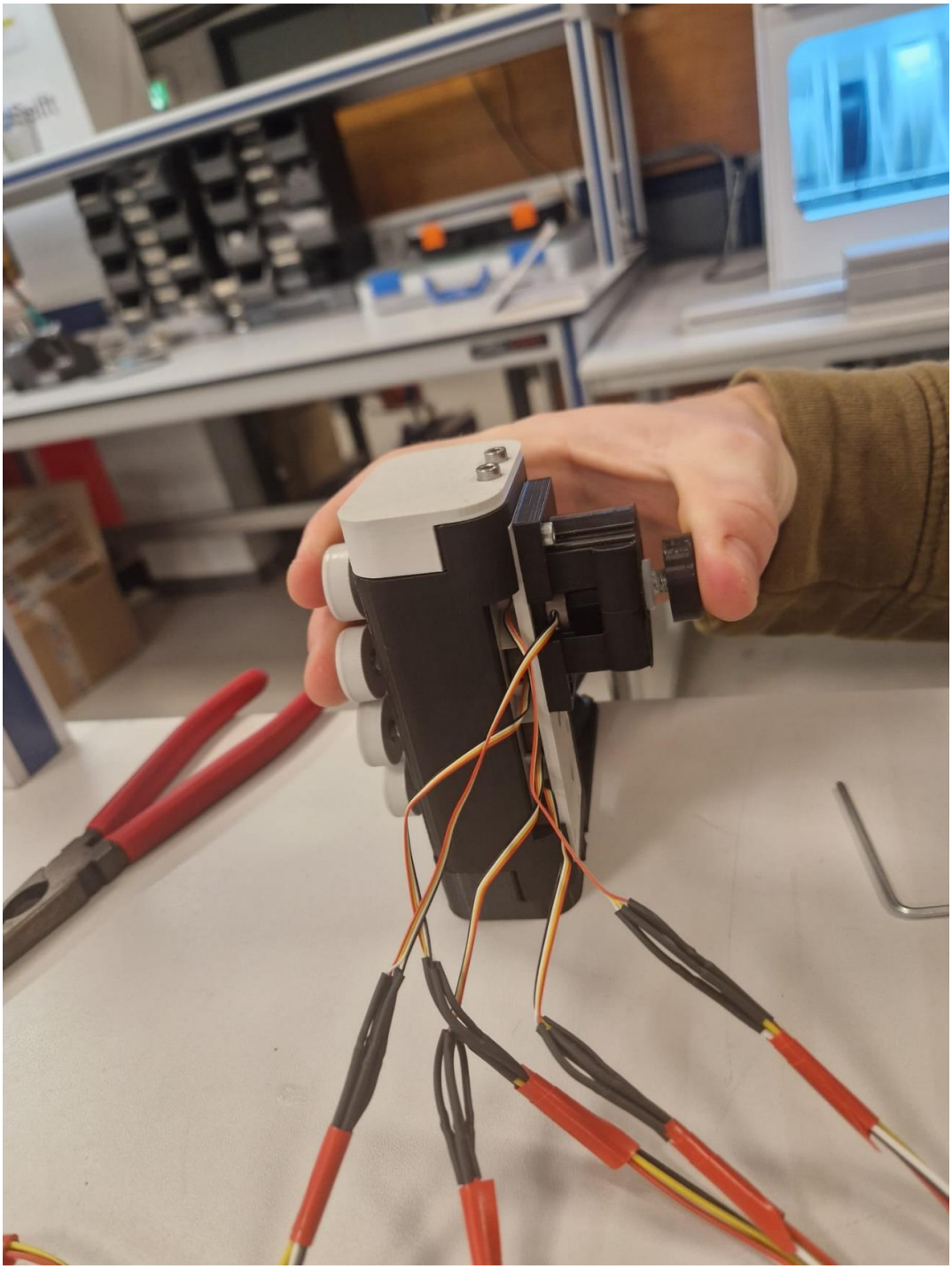

Figure 6: Precision disk grasp - device

Consent form – Hand assessment Device (Functionality & Ergonomics)

For participation in the study: 'Evaluation of a Hand Assessment Device for Measuring Finger Forces.'

Please check the appropriate box

Participation in the study	**Yes**	**No**
I have read and understood the participant information dated 10/2025. I have had the opportunity to ask questions and they were answered to my satisfaction.		
I voluntarily consent to participate in this study as a participant, and I understand that I can refuse to answer questions and that I can withdraw from the study at any time without giving a reason.		
I understand that there is no compensation for my participation.		
I understand that participation includes maximal grip trials with a conventional hand dynamometer and repeated grasp tasks (medium wrap and precision disk) on the hand assessment device, alternately with left and right hand, and a short questionnaire. All device tasks will be performed with maximum voluntary force output.		
I understand that possible risks are minimal, including mild hand fatigue or discomfort, and that I can stop the experiment at any time.		
I understand that the data collected are: device force signals, dynamometer peak values, demographic/anthropometric data (age group, sex, hand dominance, glove size), and questionnaire responses.		
I understand that my data will be pseudonymized, not linked to my name, and used exclusively for this MSc thesis. My personal information will not be shared outside the research team.		
I acknowledge that I have had the chance to ask questions and that I understand my rights as a participant.		

_____ _____ _____

Name of participant Signature Date

I, as researcher, have accurately read out the information sheet to the potential participant and, to the best of my ability, ensured that the participant understands to what they are freely consenting.

_____ _____ _____

Researcher name Signature Date

TU Delft - Faculty Mechanical Engineering (ME)
Mekelweg 2
2628 CD Delft
Tel: +31 (0)15 27 89809

APPENDIX K

ERGONOMIC DESIGN QUESTIONNAIRE

This appendix contains the full questionnaire that participants completed after the user validation session. The questionnaire assessed comfort, hand placement, stability, and overall usability of the device.

Ergonomic Design Questionnaire

Participant code: _____ Date: _____

Test condition: ☐ Precision grasp ☐ Medium wrap ☐ Power grasp

Please rate each statement below on a scale from 1 (Strongly disagree) to 5 (Strongly agree). You can add comments in the last column.

Section – Hand Placement and Fit

Statement	1	2	3	4	5	Comments
My hand could be placed naturally on the device.	☐	☐	☐	☐	☐	
The finger placement matched my natural grasp posture.	☐	☐	☐	☐	☐	
The device accommodated my hand size comfortably	☐	☐	☐	☐	☐	
My thumb and fingers aligned well with the contact surfaces	☐	☐	☐	☐	☐	

Section – Ergonomic Comfort

Statement	1	2	3	4	5	Comments
The device felt comfortable during maximum squeezing	☐	☐	☐	☐	☐	
There were no sharp edges or pressure points.	☐	☐	☐	☐	☐	
The wrist and finger posture felt natural.	☐	☐	☐	☐	☐	
The contact surfaces provided sufficient grip and stability.	☐	☐	☐	☐	☐	

Section – Grasp Experience

Statement	1	2	3	4	5	Comments
The precision grasp felt stable and natural	☐	☐	☐	☐	☐	
The medium wrap grasp felt stable and natural	☐	☐	☐	☐	☐	
The power grasp felt stable and natural	☐	☐	☐	☐	☐	
None of the grasp types caused discomfort or awkward motion.	☐	☐	☐	☐	☐	

Section – Force Application and Motion

Statement	1	2	3	4	5	Comments
The motion resistance felt consistent across repetitions.	☐	☐	☐	☐	☐	
The pistons followed my finger motion without noticeable friction or resistance.	☐	☐	☐	☐	☐	
The amount of piston travel felt appropriate.	☐	☐	☐	☐	☐	

Section –General Impression

Statement	1	2	3	4	5	Comments
The overall design feels ergonomic and intuitive.	☐	☐	☐	☐	☐	
I felt comfortable using this device for multiple trials.	☐	☐	☐	☐	☐	
The prototype device felt more natural to use than the hand dynamometer.	☐	☐	☐	☐	☐	

Open Questions

1. Which grasp felt most comfortable, and why?

2. Which grasp felt least comfortable, and why?

3. Did you notice any mechanical resistance, friction or misalignment during squeezing?

4. Do you have any suggestions to improve the ergonomic design?

5. How would you describe the main difference in feel between the prototype and hand dynamometer?

APPENDIX L
Evaluation data

This appendix presents the full group-level evaluation results for all subjects and grasp types. These results expand on the concise summary provided in the main thesis text and give a complete overview of how the device performs in terms of repeatability, accuracy, and finger-force distribution. All values shown here are based on the peak forces obtained during the 3 second maximal voluntary contraction window.

For each subject and grasp, the mean force, standard deviation (SD), coefficient of variation (CV), and root-mean-square error (RMSE) were calculated. These metrics quantify trial-to-trial consistency and allow comparison with the reference dynamometer. All statistics were computed using the total force including the thumb. The mean force excluding the thumb is also reported because this quantity corresponds directly to single-point dynamometer measurements.

This appendix contains:

- the full per-subject repeatability table,
- per-grasp precision scatterplots divided by subjects,
- group-level finger force distributions,
- and a final summary table combining SD, CV, and precision coverage for both the device and the dynamometer.

These results complement the per-subject and group summaries presented in the main text.

A. Mean, SD, CV and RMSE of the Device

TABLE VII: Per-subject repeatability metrics for all grasps. Mean_dev = device mean total force (with thumb, except in PowerGrasp, where no thumb is present); Mean_noT = device mean force excluding thumb (comparable to dynamometer values); Mean_dyn = dynamometer mean force; SD = standard deviation; CV = coefficient of variation; RMSE = root-mean-square error; n = number of trials. These values reflect only intra-subject trial-to-trial variability.

Subj	Grasp	Mean_dev (N)	Mean_noT (N)	Mean_dyn (N)	SD_dev (N)	SD_dyn (N)	CV (%)	RMSE (N)	n
1	MediumWrap	301.24	225.82	501.77	23.54	11.53	7.81	19.22	3
1	PowerGrasp	231.29	231.29	480.85	26.38	20.39	11.41	21.54	3
1	PrecisionDisk	246.42	123.71	123.56	10.09	3.40	4.09	8.24	3
2	MediumWrap	246.94	178.00	232.42	28.44	35.10	11.52	23.22	3
2	PowerGrasp	212.72	212.72	454.37	4.75	2.14	2.23	3.88	3
2	PrecisionDisk	190.59	101.82	99.70	4.74	2.94	2.49	4.10	4
3	MediumWrap	310.85	250.12	290.28	27.33	8.95	8.79	22.31	3
3	PowerGrasp	242.72	242.72	378.54	7.32	17.56	3.02	6.34	4
3	PrecisionDisk	197.09	104.26	73.88	8.22	0.48	4.17	7.12	4
4	MediumWrap	191.64	121.94	280.80	3.03	20.84	1.58	2.48	3
4	PowerGrasp	245.94	245.94	432.47	19.81	13.82	8.05	17.16	4
4	PrecisionDisk	243.23	123.64	83.03	13.62	1.30	5.60	11.12	3
5	MediumWrap	198.39	154.16	168.35	26.11	33.81	13.16	22.61	4
5	PowerGrasp	136.17	136.17	227.84	8.54	21.88	6.27	7.40	4
5	PrecisionDisk	131.93	66.65	51.65	6.63	2.55	5.03	5.74	4
6	MediumWrap	165.50	127.52	205.29	5.22	21.69	3.16	4.52	4
6	PowerGrasp	159.10	159.10	307.28	8.73	31.52	5.49	7.56	4
6	PrecisionDisk	138.28	74.27	59.82	4.09	6.03	2.96	3.54	4
7	MediumWrap	136.85	85.60	122.26	11.31	10.59	8.27	9.80	4
7	PowerGrasp	130.83	130.83	252.68	15.66	18.18	11.97	13.57	4
7	PrecisionDisk	138.15	72.23	64.07	7.26	4.61	5.26	6.29	4
8	MediumWrap	232.93	171.78	356.64	21.87	35.88	9.39	18.94	4
8	PowerGrasp	246.13	246.13	348.79	15.05	9.98	6.11	13.03	4
8	PrecisionDisk	230.00	119.37	89.57	21.04	11.42	9.15	18.22	4
9	MediumWrap	150.05	116.82	270.66	29.53	3.70	19.68	24.11	3
9	PowerGrasp	125.49	125.49	283.74	18.41	2.94	14.67	15.95	4
9	PrecisionDisk	154.76	78.89	63.09	8.24	1.74	5.32	7.13	4
10	MediumWrap	271.00	200.13	276.87	15.83	18.18	5.84	13.71	4
10	PowerGrasp	232.98	232.98	438.03	18.44	25.11	7.92	15.06	3
10	PrecisionDisk	221.96	115.27	111.14	6.86	2.94	3.09	5.94	4
11	MediumWrap	238.33	188.63	213.46	27.77	7.54	11.65	24.05	4
11	PowerGrasp	181.53	181.53	404.03	2.23	22.99	1.23	1.93	4
11	PrecisionDisk	222.71	114.37	80.74	11.30	2.55	5.08	9.79	4
12	MediumWrap	200.97	118.45	171.62	20.68	15.33	10.29	17.91	4
12	PowerGrasp	190.50	190.50	393.57	11.99	13.60	6.30	10.39	4
12	PrecisionDisk	203.29	107.85	74.53	10.08	2.90	4.96	8.73	4
13	MediumWrap	259.44	172.20	291.26	30.21	25.52	11.64	26.16	4
13	PowerGrasp	219.36	219.36	405.34	22.34	24.49	10.18	19.35	4
13	PrecisionDisk	236.73	123.28	84.34	6.81	3.83	2.88	5.90	4

B. Precision Scatterplots Per Grasp

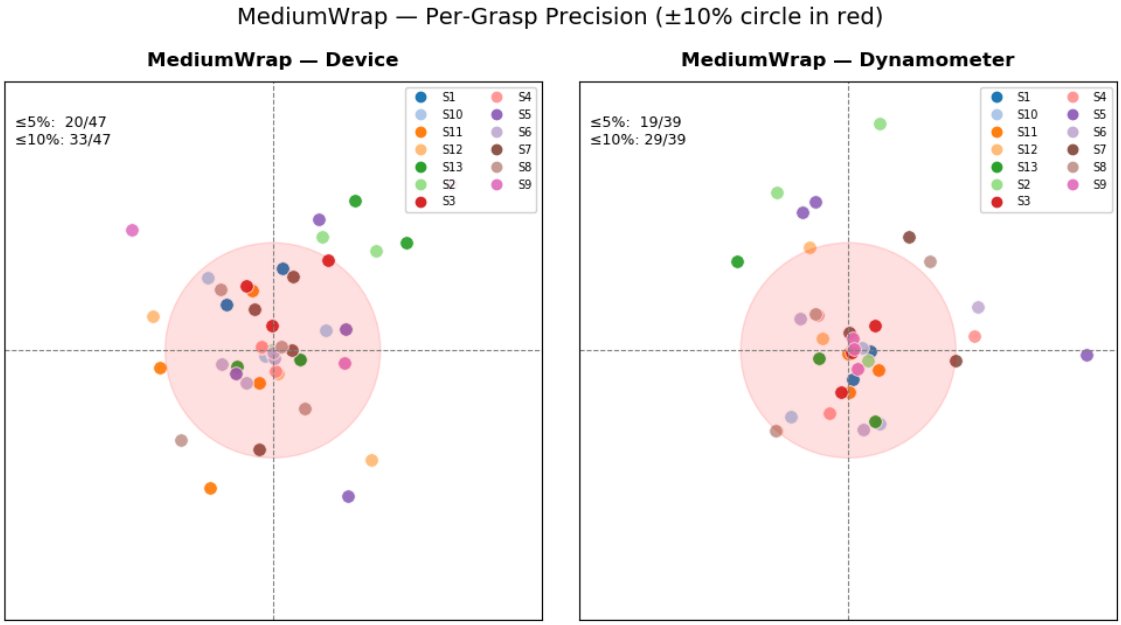

Fig. 32: Trial-to-trial precision for the Medium Wrap. Each dot represents one trial's deviation from the subject-specific mean force. The red shaded circle marks the $\pm 10\%$ boundary. Left: device results. Right: dynamometer results.

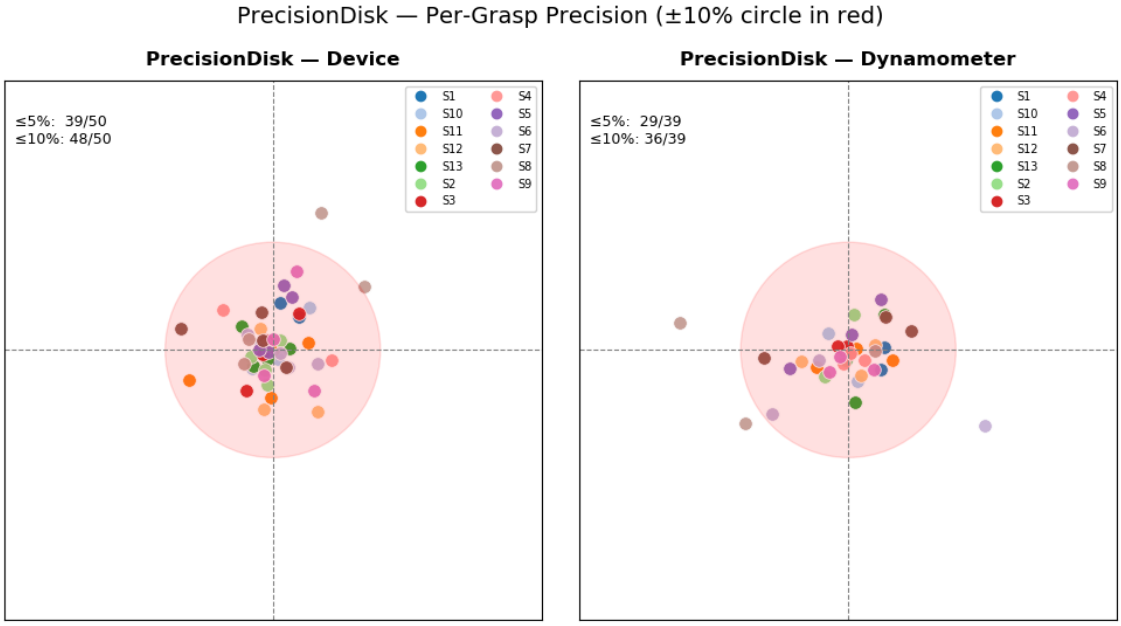

Fig. 33: Trial-to-trial precision for the Precision Disk. Each dot represents one trial's deviation from the subject-specific mean force. The red shaded circle marks the $\pm 10\%$ threshold. Left: device. Right: dynamometer.

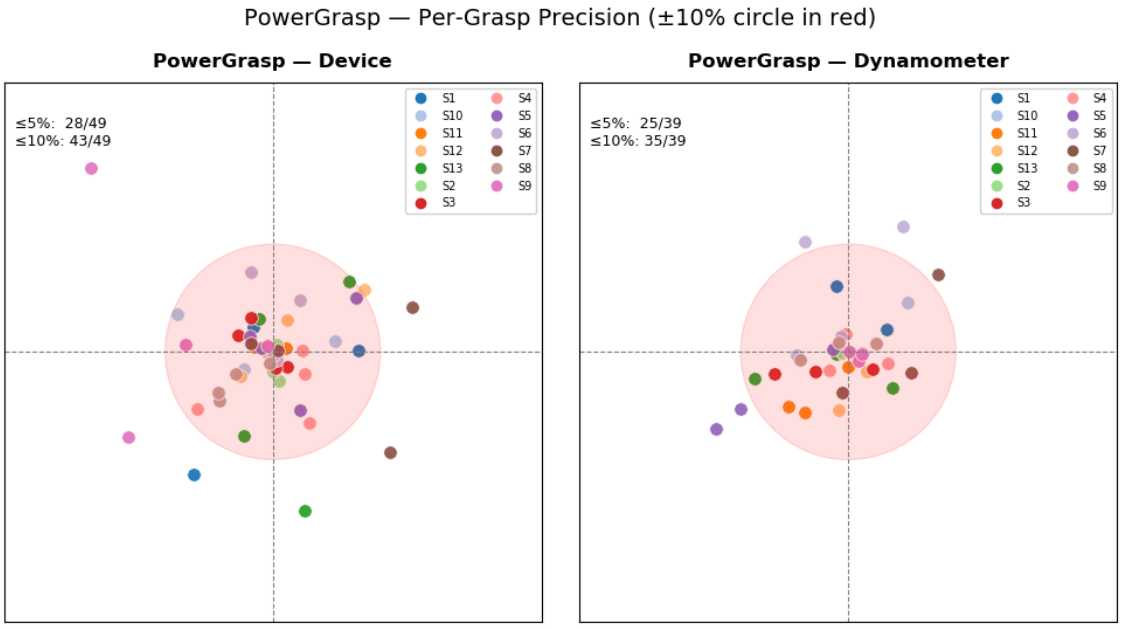

Fig. 34: Trial-to-trial precision for the Power Grasp. Each dot represents one trial's deviation from the subject-specific mean force. The red shaded circle indicates the $\pm 10\%$ threshold. Left: device. Right: dynamometer.

C. Finger Force Distribution at Peak Force

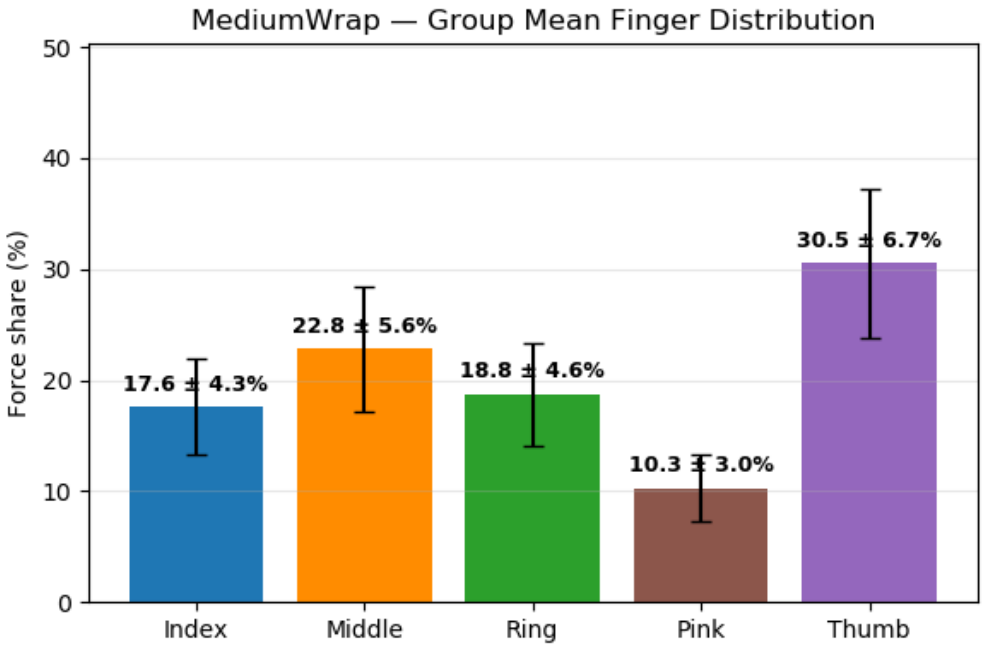

Fig. 35: Group-level finger force distribution for Medium Wrap. Bars show the average contribution of each finger to the total peak force, with error bars representing between-subject variability.

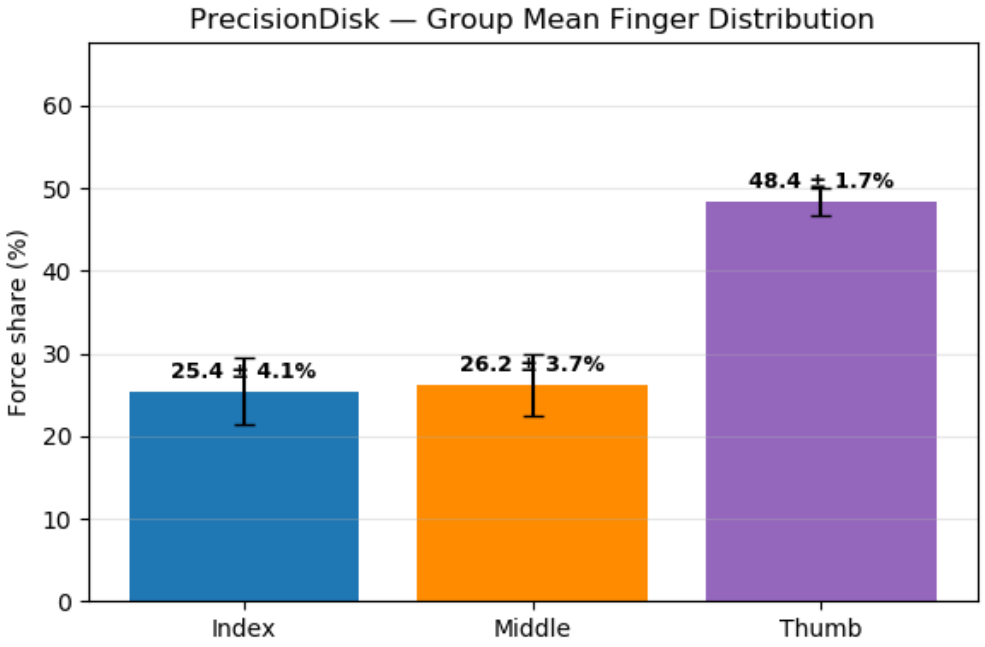

Fig. 36: Group-level finger force distribution for Precision Disk. The thumb and index finger dominate force contribution, as expected for a pinch-type grasp.

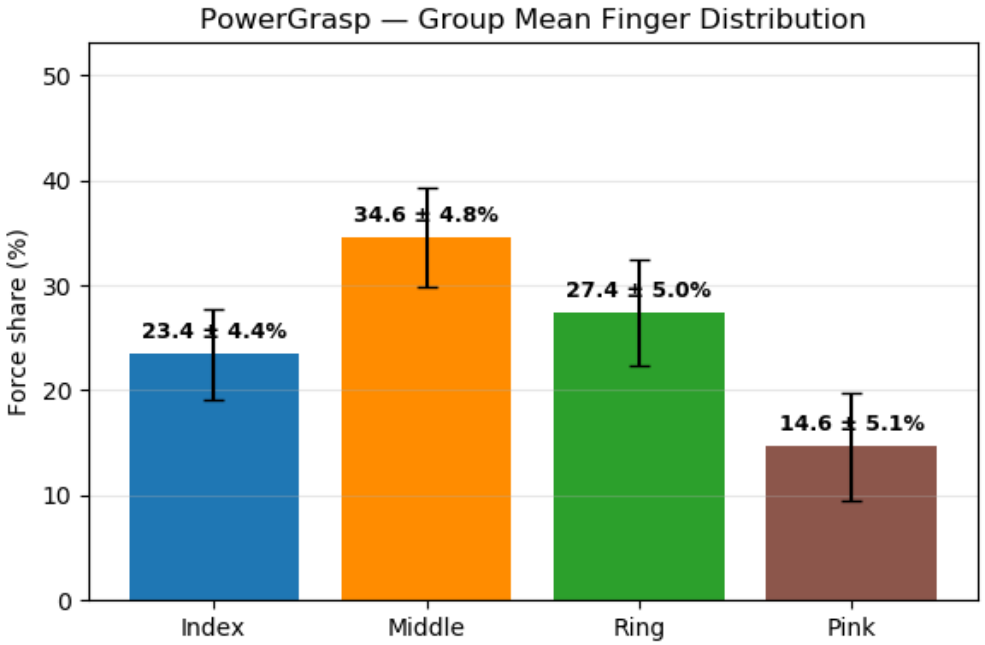

Fig. 37: Group-level finger force distribution for Power Grasp. All four fingers contribute substantially to the total force, with the middle and ring fingers contributing the most.

D. Validation Summary

Overall, the group-level results show that the device matches the dynamometer in terms of trial-to-trial repeatability, accuracy and consistency. The SD and CV values of both systems fall within the same numerical range for all grasp types, and the precision coverage results demonstrate that a similar proportion of device and dynamometer trials fall within the expected $\pm 10\%$ human repeatability band. This indicates that the device does not introduce additional measurement noise and performs on the same level as the reference instrument.

TABLE VIII: Group-level validation summary using absolute variability (SD), normalized variability (CV), and precision coverage for both the device and the dynamometer. Values represent averages across all subjects.

Grasp	**SD_{dev}**	**SD_{dyn}**	**CV_{dev}**	**CV_{dyn}**	**Dev $\leq$5%**	**Dyn $\leq$5%**	**Dev $\leq$10%**	**Dyn $\leq$10%**
MediumWrap	20.84	19.13	9.45	9.56	42.6%	48.7%	70.2%	74.4%
PrecisionDisk	9.15	3.59	4.62	5.39	78.0%	74.4%	96.0%	92.3%
PowerGrasp	13.82	17.28	7.30	5.80	57.1%	64.1%	87.8%	89.7%
Overall Mean	**14.60**	**13.33**	**7.12**	**6.92**	**59.6%**	**62.4%**	**84.9%**	**85.5%**